Rhodes Journal of Biological Sciences

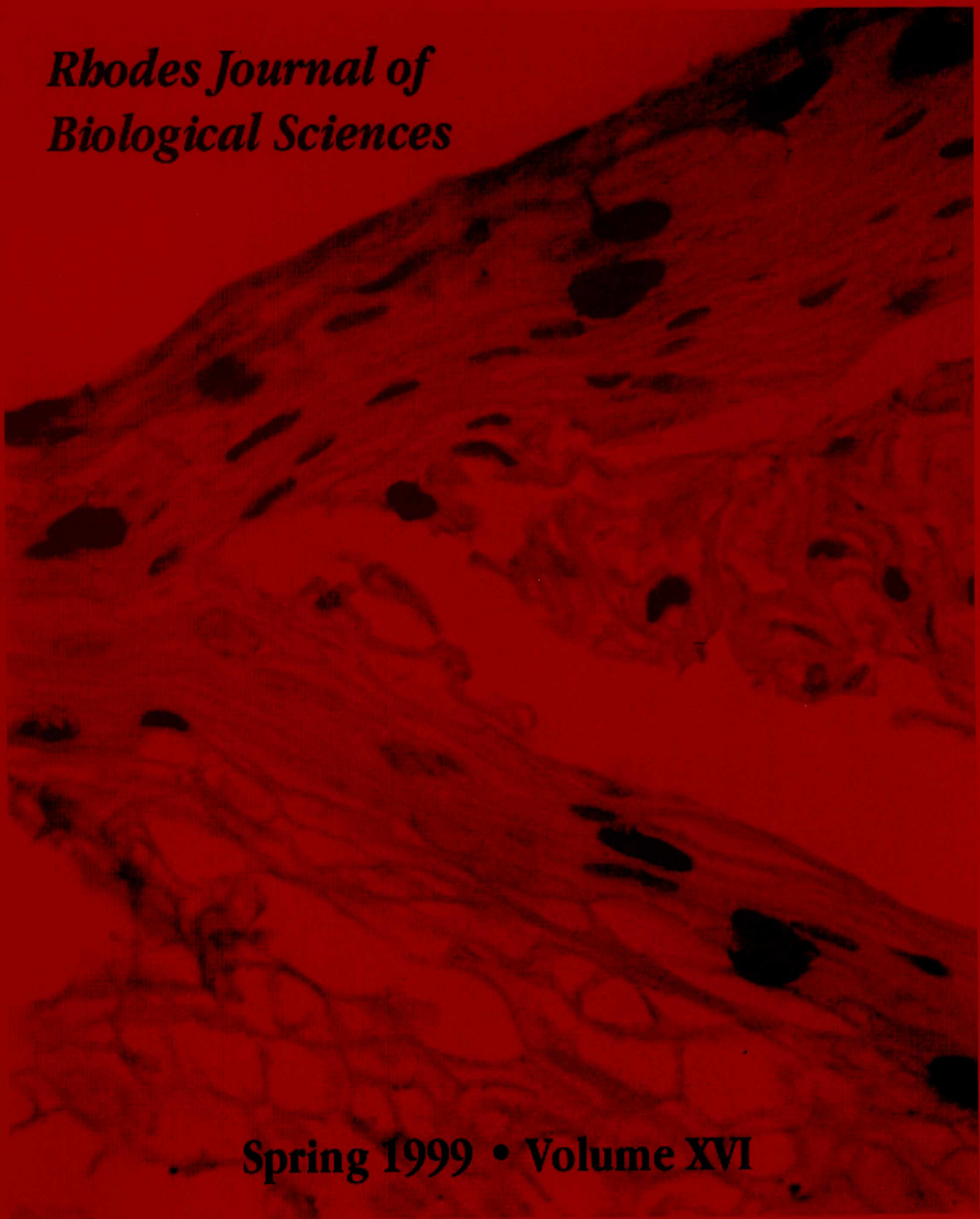

Spring 1999 • Volume XVI

Rhodes Journal of Biological Sciences

Spring 1999 • Volume XVI

Statement of Purpose: The Rhodes Journal of Biological Sciences is a student-edited, annual publication which recognizes the scientific achievements of Rhodes students. Founded sixteen years ago as a scholarly forum for student research and scientific ideas, the journal aims to maintain and stimulate the tradition of independent study. We hope that in reading the journal, other students will be encouraged to pursue scientific investigations and research.

Eric Johnson, Editor

Acknowledgements: This journal was made possible with the support of Dr. Bobby Jones and Dr. John Olsen of the Rhodes College Department of Biology. The technical assistance given by Ms. Maria Balasis was also quite valuable.

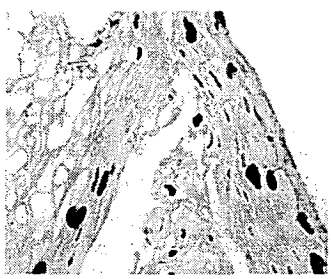

***Cover*:** The cover image is a four micron section of a formalin-fixed, paraffin-embedded section of *Condyloma acuminatum* (enlarged 400x) after DNA in situ hybridization with Human Papilloma Virus type 16 (HPV-16) DNA probes. *Condylomae* are caused by HPV infection and the nuclei of kiolocytes (dark regions) contain HPV DNA fully incorporated into the host genome.

Rhodes Journal of Biological Sciences

Table of Contents:

A Survey of the 1998-1999 Rhodes Biology Faculty

by Amy Whigham

In an effort to link the past and the present, we have surveyed the Biology Faculty about the greatest scientific advancement seen in their respective fields in the last 20 years. The opinions of the faculty provide a way for those new to the area of Biology to appreciate contributions and techniques which are considered common today in current biological research.

According to many of the faculty members, the field of molecular biology and its applications has led to great strides in other areas of study. In the opinion of Dr. Bruce Abedon, Assistant Professor, the development of these techniques has allowed "old questions to be answered and new ones to be posed". More specifically, Dr. John Olsen, Chair, proposed the application of molecular biology techniques to systematics and the study of evolutionary relationships as an integral contribution. These techniques, such as restriction mapping protocols, have opened doors which allow more direct studies of certain topics within systematics. The technology of gene cloning and gene transfers is the greatest advance within this time period, according to Dr. Bobby Jones, Professor. The development of polymerase chain reaction (PCR) method for studying DNA sequences has been significant, according to Dr. Gary Lindquester, Associate Professor. Previous molecular biology work was restricted to DNA sequences available in large quantities, and PCR has solved this problem by allowing quick amplification of small quantities of DNA. This has facilitated rapid diagnostic testing for infectious organisms and genetic defects, as well as making evolutional comparisons among organisms.

Two faculty members, Dr. Jay Blundon, Assistant Professor, and Dr. Carolyn Jaslow, Assistant Professor, stated the importance of increasing computer power. According to Dr. Blundon, "explorations into the human brain" can now be done by positron emission tomography scans and functional magnetic resonance imaging with the increased power of computers. These new technologies have "completely revised" our study and understanding of the brain and the tratment of nervous system pathologies. The appearance of powerful personal computers has also "allowed the application of engineering technology, such as strain gauges and electrode recordings" to understanding how animals functioned, according to Dr. C. Jaslow. Through the realization that actual measurements of animal functions (walking, running, etc.) could be made, the fields of functional morphology and biomechanics have emerged.

Finally, we received three additional opinions from the faculty. Dr. Alan Jaslow, Assistant Professor, believes that the "consistent use of cladistics in hypothesizing evolutionary relationships" is significant as it has "led to new understandings about vertebrate relationships" and the evolution of many character states. Ecology has made the important contribution of the "intellectually rigorous foundation from which to replace the goal of economic growth with that of sustainability, i.e., steady state conditions", in the opinion of Dr. David Kesler, Associate Professor. Dr. Lindquester also proposed that the human immunodeficiency virus (HIV) has been an important contribution in itself. In the opinion of Dr. Lindquester, HIV has served as an "eye-opener" to the idea of emerging infectious diseases, led to the enhancement of funding for

scientific research, enhanced public awareness of infectious diseases, and emphasized the need for international cooperation in the areas of public health.

As can been seen from this compilation of thoughts and opinions, the world of biology is constantly improving and leading to further advancements. Past achievements and future studies of biological research are dependent on one another, as shown by these perspectives of the Rhodes Biology Faculty.

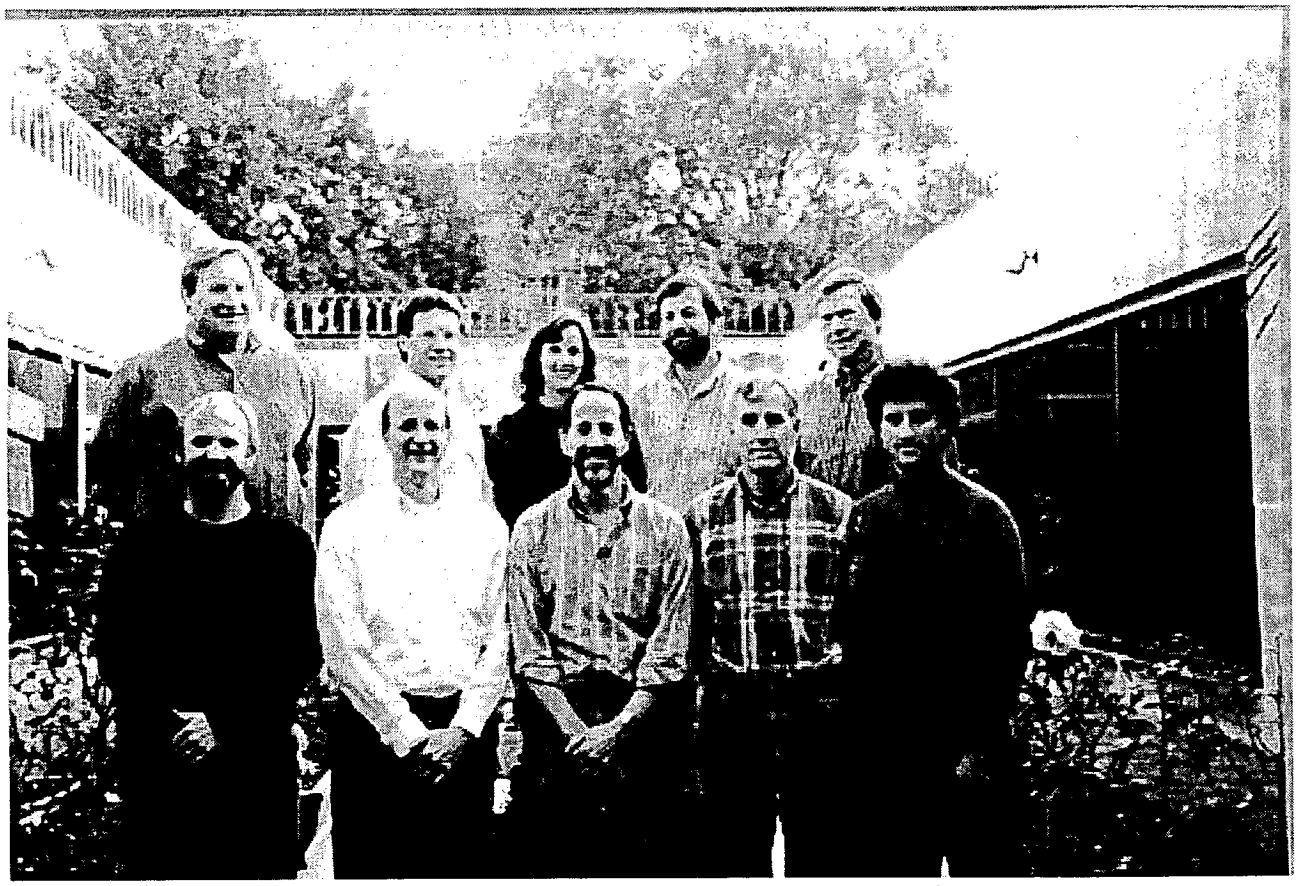

The 1998-1999 Rhodes College Department of Biology Faculty: (top left to right) Drs. Chuck Stinemetz, Gary Lindquester, Carolyn Jaslow, Alan Jaslow, Bobby Jones, (bottom left to right) Jay Blundon, John Olsen (chair), Terry Hill, David Kesler, and Bruce Abedon

Recurrent Mass Selection in *Brassica rapa* for Resistance to *Albugo candida*, Race 2, and Correlated Response in Resistance to *A. candida*, Race 7

Ford P. Baxter

Abstract:

Brassica rapa exhibits a response from selection for resistance to white rust (Albugo candida) that is indicative of a quantitatively inherited trait. Quantitative resistance may confer a general infection defense mechanism that allows for protection from all races of a particular pathogen. The objective of this study was to evaluate the impact of three cycles of mass selection for resistance to A. candida, Race 2, on resistance to A. candida, Race 7. If selection for resistance to A. candida, Race 2, also increases resistance to A. candida, Race 7, the race nonspecific resistance (RNR) hypothesis would be supported. After three cycles of selection for resistance to A. candida, Race 2, cycle 3 was significantly more resistant than the original population to both Race 2 and Race 7. Resistance to A. candida, Race 7, increased linearly with cycles of selection ($r^2 = 0.655$), as did resistance to Race 2 ($r^2 = 0.898$). All four populations (original and cycles 1-3) had higher resistance to Race 2 than Race 7, indicating the presence of race specific resistance (RSR) genes. However, the overall genotypic response to inoculation by the two races proved similar as resistance increased with subsequent generations (Pearson correlation value of 0.851). These data strongly suggest that B. rapa utilizes both RNR and RSR types of resistance.

Introduction:

Rapid-cycling Brassica populations (RCBP) were developed by Paul H. Williams and Curtis B. Hill in the 1970's with the aim of creating early flowering populations for use in laboratory conditions (1986). Recurrent selection for early flowering was carried out in the following Brassica species: B. rapa, B. juncea, B. nigra, B. napus, B. carinata, and B. oleracea. In addition to the early flowering characteristic, RCBP's contain many traits useful to breeders, including disease resistance and insect resistance.

Populations of B. rapa (2n=2x=20) exhibit a range of interaction phenotypes (IP), from resistance to susceptibility, to Albugo candida, an obligately biotrophic intercellular parasite. A. candida, also known as white rust, is an Oomycelium, producing biflagellate zoospores in sporangia borne in chains that grow along somatic hyphae, or at the tips of hyphae, and set free oospores (Agrios, 1997). While A. candida attacks the leaves, stems and flowers of many crucifers (Olds et al., 1995), the species is subdivided into many races of unique phenotype. Races are most easily determined by their different host ranges. A. candida, Race 7, is the natural pathogen of B. rapa. A. candida, Race 2 is capable of infecting B. rapa but is more prone to infect B. juncea or B. hirta in nature (Pound and Williams, 1963).

Race nonspecific resistance (RNR) is likely mediated by a large number of minor genes that act in a quantitatively inherited, as opposed to qualitatively inherited or classical Mendelian, fashion. This phenomenon of minor genes creating a major

aggregate phenotypic effect is useful for efficient protection of a crop from all races of a pathogen. Plant populations that have undergone selection for RNR should exhibit a significant increase in resistance to all races of a particular pathogen. Edwards and Williams (1987) performed three cycles of mass selection of B. rapa for resistance to A. candida, Race 2, and observed a significant increase in resistance over cycles, indicating that this trait is responsive to selection. Because no major resistance genes existed in the original population, the authors suggested that this resistance is quantitatively inherited. Abedon and Williams (unpublished data) investigated the levels of resistance to A. candida, Race 2, and A. candida, Race 7. Significant increases in resistance to both races occurred over two cycles, indicating this resistance may be race nonspecific. However, there was poor correlation between the mean interaction phenotypes (IP) of each race. Resistance to Race 2 increased linearly over cycles (C_0=2.8, C_1=1.9, C_2=1.7, r^2 = 0.85). For A. candida, Race 7, inoculation, the C_1 generation actually showed decreased resistance to A. candida, Race 7 (C_0=4.6 , C_1=5.1, C_2=3.5 , r^2 = 0.85). Though the C_2 generation was more resistant to A. candida, Race 7, than the C_0 generation, additional study is needed to confirm if an association between Race 2 and Race 7 actually exists. Abedon and Williams (unpublished data) also found that in each cycle, plants were more susceptible to Race 7 than Race 2. This indicates that some race-specific resistance (RSR) genes exist in this species.

This study will determine if RNR exists in B. rapa by evaluating if a correlated response in resistance to A. candida, Race 7, occurred after three cycles of recurrent selection for resistance to A. candida, Race 2.

Materials and Methods:

The C_0, C_1 and C_2 populations developed by Edwards and Williams (1987) were obtained from the Crucifer Genetics Cooperative (CGC) (catalogue numbers for C_0, C_1, and C_2, are 1-6, 1-2, and 1-3, respectively). Details of the selection process used to make cycle 1 and cycle 2 are available in Edwards and Williams (1987). We selected a third cycle (cycle 3) for this study because cycle 3 was not available from the CGC. The selection method used was a modification of that devised by Edwards and Williams. Two hundred and fifty seeds of cycle 2 were planted for each cycle of selection, in 2.54 cm^2 cells (200 cells/tray) containing Jiffy Mix (1:1 Canadian sphagnum peat and vermiculite, produced by Jiffy Products of America, Inc). Overplanting ensured at least 200 plants were available for selection. Continuous illumination was provided with Phillips TC70 fluorescent bulbs. Soil moisture was maintained through a felt wicking system devised by the CGC that enables all the plants within a particular tray to receive exactly the same level of water and nutrients. Distilled water was used for the first three days after planting. Beginning with day 4, 50% Hoagland's solution (Sigma Chemical Co.) was maintained in the wicking basin.

The disease screening process for A. candida infection of Cruciferae was outlined by Williams (1985). Sporangia of A. candida, Race 2, obtained from the CGC (no catalogue number available) were incubated for two to three hours at 160C, until they became motile. With the aid of a hemacytometer, a zoospore suspension 1-2 x 105 spores/mL was obtained. A 10 µL drop of inoculum was placed on the adaxial surface of each cotyledon five days post-germination. High humidity was maintained after

inoculation by placing a black plastic tray over the plant-containing tray. After 12 hours (270C), the top tray was removed and droplets were allowed to dry with light-bench lights off to avoid burning the leaves. The IP was assessed seven days after inoculation using the IP scale devised by Williams (1985) (Figure 1). The scale ranges from 0 (no reaction) to 9 (very few pustules on upper surface, many large coalescing pustules on lower surface). The infection intensity is rated higher when fungal sori are on the abaxial surface, because the drop of inoculum is placed on the adaxial surface and the infection progresses through the cotyledon.

Figure 1: IP Scale (Williams, P.H. 1985. White Rust Disease Screen - Albugo candida. Crucifer Genetics Cooperative.)

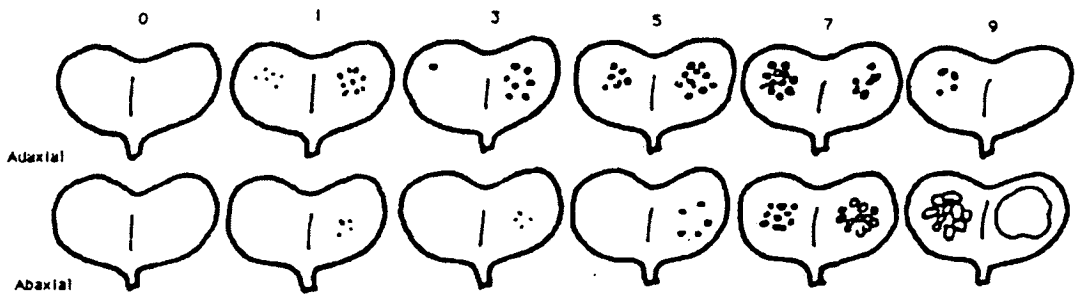

Plants with the lowest IP's were selected out (18% selection intensity) and randomly cross-fertilized so that the progeny produced would best represent the entire selected subpopulation and minimize inbreeding distortion. It was expected that the progeny would exhibit more resistance, and that determination was made by controlling for environmental noise and applying statistical analysis.

In order to have enough seed available for evaluating response to selection, all four populations were increased. For each population, ~250 plants were randomly pollinated. Siliques were collected from each plant and a balanced bulk of equal genetic representation among individual plants was made for each population. The increased populations then represented all the variability of their parent populations.

The four populations - C_0, C_1, C_2, and C_3 - were grown in a randomized complete block design (RCB) with 10 replications. One block consisted of one tray. A cross-classified experimental design was used with populations each receiving two inoculation treatments for a total of eight treatments evaluated per tray. Each treatment was planted in on 10-cell row. Cells were overplanted with seed and thinned to one plant/cell prior to inoculation. For each tray, only the eight middle rows, of an available 20, were used to allow for maximum and constant light coverage from the light bench.

Within each block, one row of a particular population was inoculated with A. candida, Race 2, the other with A. candida, Race 7, as dictated by the randomization used in planting the rows. These races, initially obtained from the CGC, were increased by inoculating an original population and collecting the resulting spores. After the plants were infected, they were evaluated on the IP scale of Williams (1985).

Analysis of variance (ANOVA) allowed the variance associated with main and interaction effects to be separated. Statistics were based on the mean IP for all plants in a row. Regression analysis was performed to determine responses to selection. The

Pearson correlation was used to determine the relationship between resistance to Race 2 and resistance to Race 7, across cycles. A p-value of at least 0.05 was used to determine all significance levels.

Results and Discussion:

Genotype and race effects were significant ($p < 0.01$). Block effects were not significant, indicating similar environments for each tray. This was expected given the controlled lab environment and is one of the advantages of using Fast Plants.

Recurrent selection for three cycles produced significantly differentiated genotypes in terms of resistance to both Race 2 and Race 7. For Race 2 the significance reached the 0.01 level (Table 2), while for Race 7 significance was at the 0.05 level (Table 3). The Race 7 variance was probably not as large because the trend over cycles was not as well defined, due in large part to the fact that C1 increased in susceptibility compared to the original population. Table 4 and Graph 3 show that the regression coefficient (r^2) for the four genotypes inoculated with Race 7 was 0.655 (not statistically significant). Actually, at 0.898, the regression coefficient for Race 2 IP is not statistically significant either, but it is different from the Race 7 IP and in the direction of a straighter line (Graph 2). Race 2 IP's strong trend indicates strong progress from selection. Race 7 IP did not match a linear decline in IP as well, due in large part to the anomalous C1 behavior. A linear decline in degree of infection follows the typical response to selection seen in additive quantitative traits. The regression lines for both the Race 2 IP's and Race 7 IP's were strongly negative, as IP decreased in response to selection for resistance. At -0.818, the slope for Race 2 IP was very close to being statistically significant, at $p = 0.052$ (Graph 2 and 3).

But while a significant amount of variation did exist in these populations, there was a strong correlation in resistance to Race 2 and Race 7, supporting the RNR hypothesis ($r^2 = 0.851$). This is despite the anomaly of C_1 having decreased resistance compared to C_0, which was also observed in the Abedon and Williams study (unpublished data). Though correlated, an order of magnitude difference exists in mean IP's for the differentially inoculated groups. Graph 1 shows the trend of mean IP value for Race 2 and Race 7 overlaid and clearly illustrates how plants selected for resistance to Race 2 had significantly increased resistance to Race 7, over cycles. Resistance to Race 2 was greater than resistance to Race 7 for each cycle of selection (Table 4, Graph 1). Abedon and Williams (unpublished data) also found the A. candida, Race 7 IP's to be greater than the Race 2 IP's. This indicates that RSR genes do exist in B. rapa and are responsible for the differential host ranges of the races, and that RSR is not mutually exclusive with RNR. This is an expected result given that Race 7 is the natural pathogen to B. rapa, to which B. rapa naturally has fewer resistance genes than for Race 2.

Though progress from selection for resistance is not significantly linear, a genetic trait need not show linearity in phenotype through selection. Selection for three cycles of resistance to A. candida, Race 2 does yield significantly different genotypes as indicated by differential resistance phenotype to Race 2 and Race 7 A. candida. The presence of a strong, though not significant, correlation between the Race 2 and Race 7 IP's of the four populations demonstrates the strength of the RNR hypothesis. However, the demonstration that selection yields significantly different genotypes trending in the

direction of resistance is all that is necessary to support the RNR hypothesis, because this indicates selection over cycles to Race 2 has produced a significantly different Race 7 IP.

The genes involved in RNR may code for general defenses such as cell wall thickness, cuticular layer thickness, or wax production. Abedon and Williams have found some morphological changes associated with selection for resistance to A. candida, Race 2, including a decrease in cotyledon width and plant height, and a delay in days to anthesis. These could be pleiotropic effects associated with selection, however, rather than indicative of the mode the plants employ to achieve resistance. Electron micrograph studies of structural changes at the cellular level over generations might elucidate resistance mechanisms.

Results:

Table 1: ANOVA of C_0, C_1, C_2, and C_3 Populations

Source of Variance	Degrees of Freedom	Mean Square
Genotype	3	18.169**
Race	1	85.657**
Block	9	1.522 **NS**
Genotype X Race	3	1.743 **NS**
Genotype X Block	27	1.778 **NS**
Race X Block	9	1.568 **NS**

*,** = Significant at 0.05 and 0.01 probability levels, respectively.
NS = Not significant

Table 2: ANOVA of C_0, C_1, C_2, and C_3 Populations Inoculated with A. candida, Race 2

Source of Variance	Degrees of Freedom	Mean Square
Genotype	3	12.411**
Block	9	1.476 **NS**

*,** = Significant at 0.05 and 0.01 probability levels, respectively.
NS = Not significant

Table 3: ANOVA of C_0, C_1, C_2, and C_3 Populations Inoculated with A. candida, Race 7

Source of Variance	Degrees of Freedom	Mean Square
Genotype	3	7.501*
Block	9	1.615 **NS**

*,** = Significant at 0.05 and 0.01 probability levels, respectively.
NS = Not significant

Table 4: Regression Analysis and Correlation of Mean IP's for C_0, C_1, C_2, and C_3 Populations

Genotype	Mean Race 2 IP	Mean Race 7 IP
C_0	4.344 ± 1.1095	5.802 ± 1.9575
C_1R	4.2780 ± 1.5587	6.177 ± 1.2794
C_2R	2.7050 ± 0.4000	5.576 ± 1.4726
C_3R	2.1420 ± 1.0912	4.192 ± 1.1953
Coefficient of determination (R^2)	0.898 NS	0.655 NS

Pearson Correlation	0.851 NS

*,** = Significant at 0.05 and 0.01 probability levels, respectively.
NS = Not significant

Graph 1: Comparison of the Effects of Recurrent Selection for Resistance to Race 2 on Race 2 IP vs Race 7 IP

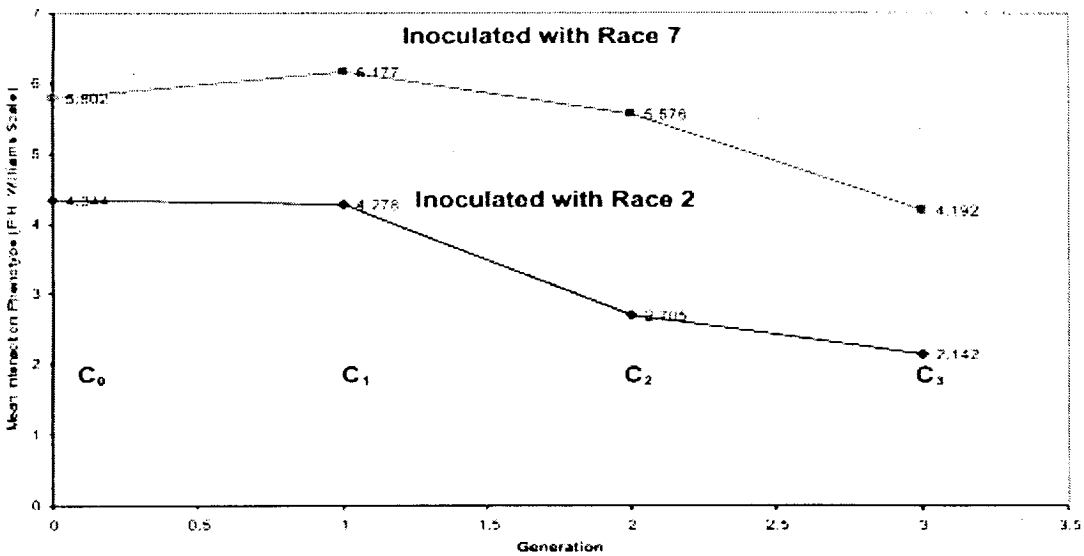

Graph 2: Regression Analysis: Progress From Three Cycles of Selection for Race 2 Resistance as Evidenced by Race 2 IP

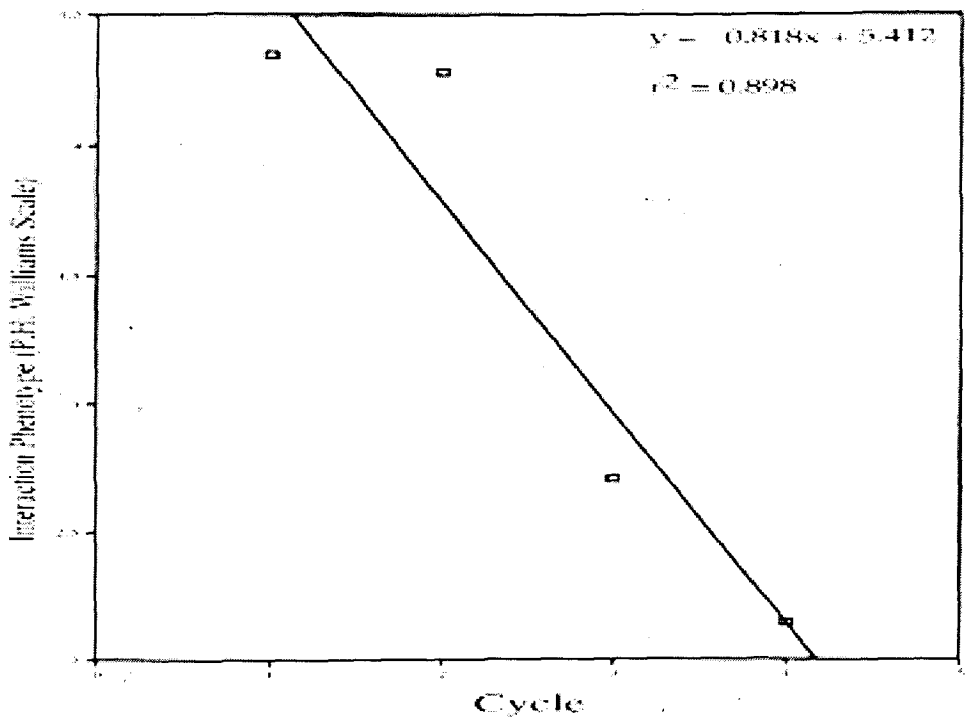

Graph 3: Regression Analysis: Progress From Three Cycles of Selection for Race 2 Resistance as Evidenced by Race 7 IP

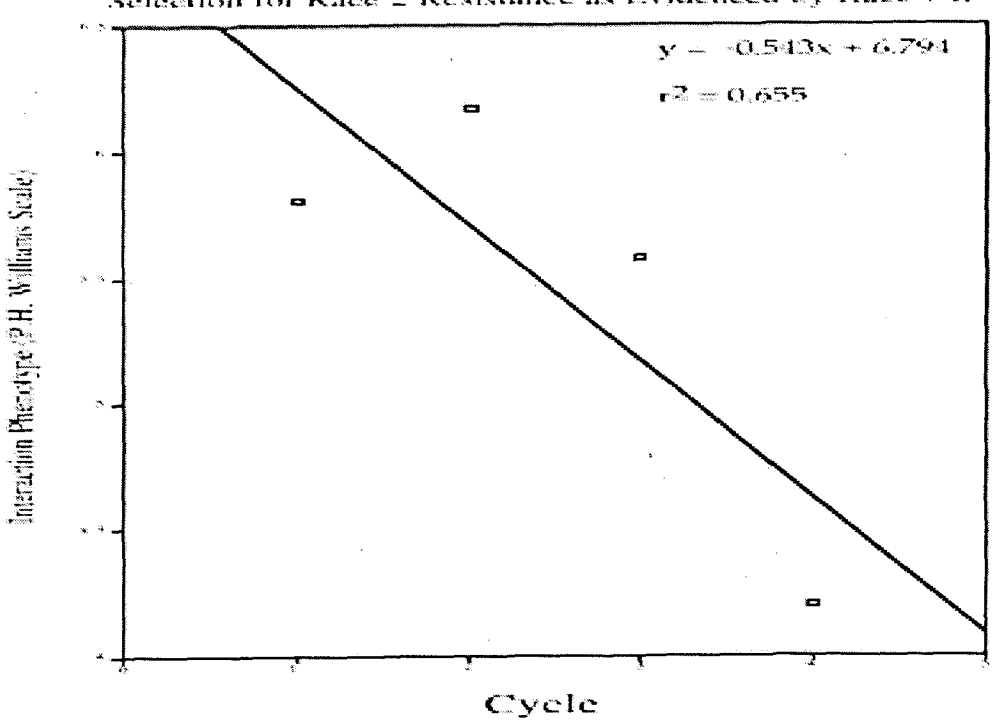

References:

Agrios, G.N. Plant Pathology, 4th ed. New York: Academic Press, 1997.

Edwards, M.D., and P.H. Williams. Selection for Minor Gene Resistance to Albugo candida in a Rapid-Cycling Population of Brassica campestris. Phytopathology. 77:527-532.

Olds, T.M., et al. 1995. Genetics of Brassica rapa (syn. campestris). 2. Multiple disease resistance to three fungal pathogens: Peronospora parasitica, Albugo candida and Leptosphaeria maculans. J. Hered. 75:362-369.

Pound, G.S., and P.H. Williams. 1963. Biological Races of Albugo candida. Phytopathology 53:1146-1149.

Williams, P.H., and C.B. Hill. 1986. Rapid-Cycling Populations of Brassica. Science. 232:1385-1389.

Development of an RT-PCR-Based Diagnostic Assay for EHV2

E. Amanda Johnson, under guidance of Dr. Gary J. Lindquester

Abstract:

Equine herpesvirus 2 is a gamma herpesvirus infecting up to 89% of some horse populations that has been linked to such diseases as conjunctivitis, upper respiratory tract disease, and general malaise. In order to establish a causal relationship between the disease and its suspected symptoms, however, it is necessary to develop a reliable diagnostic assay that can distinguish an active infection from one that is lying latent. Using polymerase chain reaction (PCR) technology, we have developed an assay that screens for the production of viral glycoprotein B (gB) within the infected rabbit kidney cells. The viral RNA is isolated, converted into copy DNA (cDNA) using reverse transcriptase, and amplified with PCR using primers specific for gB. Subsequent examination of the PCR products on agarose gel electrophoresis reveals either the presence of gB, indicating an active EHV2 infection, or its absence, indicating that the disease is either lying latent or the cell is not infected. The direction of future research will be toward applying this technique to samples from horses suspected of infection.

Introduction:

Equine herpesviruses 2 and 5 (EHV2 and EHV5) are gamma herpesviruses, a class typified by Epstein-Barr virus, the virus that causes mononucleosis in humans (1). Infection rates for EHV2 are as high as 89% in some equine populations, based on nasal cavity and leukocyte isolations (2). In addition, the virus has been linked to poor performance in older horses, and also in younger horses when they are first introduced to racing stables (1). EHV2 has been implicated in upper respiratory tract disease, conjunctivitis, general malaise, and immunosuppression in foals (3, 4, 5, 6). Equine herpesvirus 2 has the ability to lie latent in lymphoid tissue, such as B cells, and pulmonary macrophages (7), and thus is a candidate for the cause of such unexplained illnesses as conjunctivitis and respiratory tract infections in otherwise normal horses.

A diagnostic assay for EHV2 is a necessity for the establishment of a causal relationship between EHV2 and the symptoms for which it is thought to be responsible. Antibody titer assays, which are the standard for indicating a specific viral infection, are useful for indicating an equine herpesvirus infection of type 2 or 5, but there are two problems with this kind of assay. First, EHV2 and EHV5 are antigenically similar, and thus distinguishing between antibodies raised against them is very difficult. Second, in the case of EHV2 and EHV5, a test for the presence of antibody to the virus in the blood cannot differentiate between an active and latent infection, since those antibodies are always in circulation. Therefore, it is necessary to develop a specific diagnostic assay for EHV2 that can differentiate between latent and productive infections.

Polymerase chain reaction (PCR) is a method of specifically amplifying certain sequences of DNA, using a heat-resistant DNA polymerase and primers to replicate the DNA strand, producing thousands of copies (8). Any PCR-based assay for a reactivated EHV-2 infection, because of its ability to lie latent, must be able to distinguish actively

replicated genes from those that are merely lying latent. PCR is a method that will allow analysis of the DNA present within a cell, but the DNA for EHV-2 will always be present in an infected horse, and thus is not specific for a reactivated infection. Viral RNA, however, is only present when there is production of viral proteins, i.e., in a symptomatic infection. In order to amplify an RNA sequence by PCR, it is necessary to convert it to DNA by using reverse transcriptase.

The sequence amplified in the assay must be one that is ubiquitous for all strains of EHV2, but may be easily differentiated from EHV5. Glycoprotein B (gB) is an envelope protein that is required for infectivity and functions in the penetration of the virus into cells by promoting the fusion of the virion and plasma membranes (9). It is the most highly conserved protein of the herpesvirus family (9), so that there is a very low mutation rate within a particular strain. If the primers used in the RT-PCR reaction are specific to gB from EHV2, an isolation and analysis of RNA could be used to discern active production of gB. This production of gB would therefore indicate that the horse was undergoing an active EHV2 infection.

Materials and Methods:

Cell culture: RK-13's (ATCC; Manassas, VA) were cultured in MEM (Sigma; St. Louis, MO) with 10% FBS, 23mM HEPES, 26mM monobasic sodium bicarbonate, which was adjusted to a pH of 7.5. RK-13's were plated in a T-75 flask, and fed every other day.

Virus infection: RK-13's were infected when they had reached about 80% confluency with three different strains of EHV2: T2, 86, and 1-141 (supplied by G.J. Lindquester, from Australia). They were infected by removing the culture medium and covering the monolayer with 0.5mL of viral stock (made by freezing culture medium of infected cells at -80°C), and incubated at 37°C for 1 hour. At the end of the initial incubation period, the cells were covered with 15mL's of maintenance medium (MEM, 1% FBS, 23mM HEPES, and 26mM $NaHCO_3$). The flask of control cells were covered with 0.5mL's of maintenance medium during the initial incubation, and then treated the same as the infected cells. The medium on all flasks was changed every other day until cytopathic effects (CPE) became evident.

RNA isolation: Isolations were done on cells in the mid stages of CPE, as well as in the last stages. The denaturing solution was prepared according to the method of Chomczynski and Sacchi (10), implementing the isolation protocol of Meltzer, et al (11). The suspended RK-13's were placed into a 15mL conical vial and rinsed once in ice-cold phosphate-buffered saline (PBS). The cells were resuspended in 1.2mL of denaturing solution and homogenized in a Dounce homogenizer (5-6 strokes). After adding 120µL of 2M sodium acetate and 1.2mL of phenol-chloroform-isoamyl alcohol (in a microfuge tube) and shaking for 15s, the sample was chilled on ice for 15 minutes. The sample was centrifuged at 10,000 rpm for 15 minutes, and 1 volume of isopropanol was added to the aqueous phase. The sample was chilled and centrifuged again, the isopropanol was removed, and 1mL of ice-cold 70% ethanol was added. After another centrifugation, the ethanol was poured off and the pellet was resuspended in 20µL of DEPC-treated water.

DNase treatment of RNA: RNA samples were DNase-treated to remove any lingering DNA from the RNA isolation. 15µL of the RNA isolate was mixed with 1µL of 1:10 DNase (Boehringer-Mannheim; Indianapolis, IN) in a microfuge tube, which was then incubated at 37°C for 15 minutes. The volume was then brought up to 100µL with water, and 100µL of phenol-chloroform-isoamyl alcohol was added; the tube was inverted 20 times to mix. The sample was centrifuged at 15,000 rpm for 30 seconds to separate the aqueous and organic layers. The aqueous phase was removed, transferred to a clean tube, and the volume was brought up to 100µL with water. After repeating the DNase treatment in the same manner, a half a volume of 7.5M ammonium acetate and 2.5 volumes of 100% ethanol were added. This mixture was incubated at –80°C for 15 minutes, and then centrifuged at 15,000 rpm for 15 minutes. The ethanol and ammonium acetate mixture was poured off, the pellet was rinsed in 150µL of 70% ethanol, centrifuged as before, and resuspended in 20µL of DEPC-treated water.

Production of a gB RNA transcript: The gB DNA sequence was inserted into a vector, pGEM® (Promega; Madison, WI), and was transcribed into RNA, in order to produce a gB RNA transcript that could be used as a positive control for the reverse-transcription reaction. The transcription reaction used 20 units of T7 RNA polymerase (Boehringer-Mannheim) to 1µg of pGEM.gB (Promega), 20 units of RNase ribonuclease inhibitor, and equal amounts ATP, CTP, UTP, and GTP (100µM) The reaction was carried out in transcription optimized buffer, and incubated at 37°C for 90 minutes. The products were diluted to various concentrations and used as template in RT-PCR to test the success of the transcription reaction (data not shown). They were also used as a positive control for the reverse transcription reaction.

PCR reactions: The master mix was formulated using the concentrations recommended by Promega, and Promega provided all reagents. Each reaction was carried out in Taq buffer and contained 0.1 unit of themostable Taq polymerase, 100 µM concentrations of each of the nucleotides, and the following primers: E2.5, forward 5' TGATAACGCTA-CCAGATTCTTTGC 3' and E2.7, reverse 5' TTGCTCAGCTCGTACCACATG-AGCG 3' (25µM each). The primers used were manufactured by Gibco (Gaithersburg, MD) for Dr. G. Lindquester in April of 1997. Four µL of sample was used in each reaction.

RT-PCR reactions: The reaction mixture was formulated using the concentrations recommended by Promega and Promega provided all reagents. Each reaction contained 0.1 unit of Taq polymerase, 100 units of reverse transcriptase, M-MuLV (Boehringer-Mannheim), 25µM concentrations of each of the primers, and was carried out in reverse transcriptase buffer. Four µL of template was added to each reaction.

RT-PCR conditions: RT-PCR was performed in a single step, using the DNA Engine PTC-200, Peltier Thermal Cycler (MJ Research; Watertown, MA). The reverse transcription was carried out at 42°C, for 30 minutes. There were 30 PCR cycles, with temperatures and times as follows: denaturing-95°C for 1 minute; annealing-60°C for 1 minute; transcription-72°C for 1 minute.

Electrophoresis conditions: Samples (10uL of RT-PCR product + 2uL red juice) were on a 2% agarose gel. The gel was then stained with ethidium bromide for 30 minutes, and destained for 30 minutes. The gel was then visualized under UV light and photographed.

Results and Discussion:

Rabbit kidney cells infected with T2 showed CPE within 5 days, at which time they began forming syncitia and cleared patches. Within 9 days, the cells were only ~5% confluent. Cells infected with 86 began showing CPE within 3 days, at which time they began forming syncitia and aggregations. The syncitia were mostly dead by the fifth day, with cleared patches beginning to form. The cells were still 20% confluent on the eighth day, and most of the cells were in suspension on the twelfth day. Cells infected with 1-141 began showing CPE within 3 days, at which point they began to clear slightly. This process continued, until they were only about 4% confluent on the eighth day (see pictures). The flask of control cells remained healthy, but crowded, until the sixth day, at which point they began lifting off the monolayer. On the eighth day, they were about 20% confluent, and resembled the flask of cells infected with T2.

When RT-PCR was performed and the samples were run on a gel, the results were encouraging (see figure 1). All isolations from infected RK-13's produced bands of glycoprotein B, which correspond to the bands produced at the positive controls. This indicates that strain heterogeneity makes no difference in the sensitivity of the assay, since the band is seen in all strains. The absence of glycoprotein B in the uninfected cells suggests that this kind of assay is indeed specific for cells infected with EHV2.

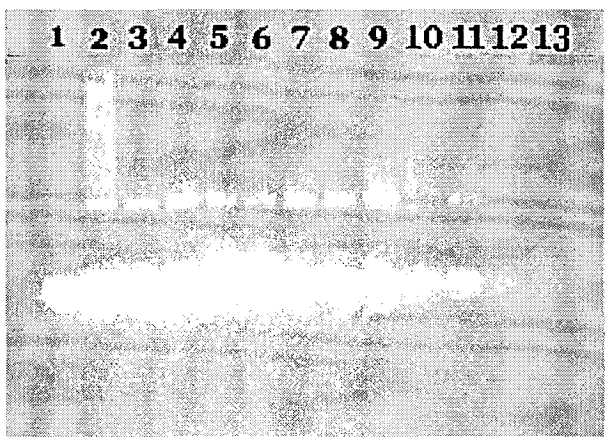

Figure 1: Agarose gel electrophoresis of RT-PCR products. 1: Water (negative control); 2: Mid-CPE T2; 3: Late-CPE T2; 4: Mid-CPE 86; 5: 1:100 gB RNA (+ control); 6: 1:1000 gB DNA (positive control); 7: Late-CPE 86; 8: Mid-CPE 1-141; 9: Late-CPE 1-141; 10: Uninfected RK-13 RNA; 11: gB RNA and mid-CPE 86 (2uL of each); 12 (only PCR): gB RNA; 13 (only PCR): Late-CPE T2.

The smear seen in the band that corresponds to the T2 isolation during the mid-stages of CPE is a result of leftover genomic DNA, although lane 13 indicates that the DNase treatment was successful. The problem of residual genomic DNA has been

persistent, and revision of the protocol may prove necessary in order to correct it. If the samples were exposed to more repetitions of DNase treatment the residual DNA, we might be able to dissolve and extract the residual DNA. It is possible that simply homogenizing the cells more at the very beginning would shear the high molecular weight DNA molecules such that they would be easier to remove. A second treatment with guanidinium thiocyanate, further denaturing the DNA, might also eliminate some of the residual DNA.

The extra bands, below the band corresponding to gB, seen in the two positive controls could be what are known as "primer dimers." These may result when the concentration of template is below a certain critical level, which may be determined experimentally. If these bands are indeed the result of a low template concentration, then their presence should be able to be repeated in the experimental lanes by simply lowering the concentration of template added.

The next logical steps in the development of this assay include verifying the results and extending its scope. The products of the RT-PCR reaction should be digested with restriction enzymes to ensure that the glycoprotein B harvested corresponds with the published pattern. In addition, quantitation of the RT-PCR products would allow us to determine the beginning of transcription of late genes within the infection cycle.

References:

1.) Telford, E.A.R., M.J. Studdert, C.T. Agius, M.S. Watson, H.C. Aird, and A.J. Davison. Equine Herpesviruses 2 and 5 are g-Herpesviruses. *Virology* **195**: 492-499.

2.) Roeder, P.L. and G.R. Scott (1975). The prevalence off equine herpes virus 2 infections. *Veterinary Records* **96**: 404-405.

3.) Studdert, Michael J. (1971). Equine herpesvirus 4: concurrent infection in horses with strangles and conjunctivitis. *Australian Veterinary Journal* **47**: 434-436.

4.) Blakeslee, J.R., R.G. Olsen, E.S. McAllister, J. Fassbender, and R. Dennis (1975). Evidence of respiratory tract infection caused by equine herpesvirus type 2, in the horse. *Canadian Journal of Microbiology* **21**: 1940-1946.

5.) Palfi, V., S. Belak, and T. Molnar (1978). Isolation of equine herpesvirus type 2 from foals, showing respiratory symptoms. *Zentralblatt für Veterinärmedizin Reihe B* **25**: 165-167.

6.) Sugiura, T., Y. Fukuzawa, M. Kamada, Y. Ando, and K. Hirasawa (1983). Isolation of equine herpesvirus type 2 from foals with pneumonitis. *Bulletin of the Equine Research Institute* **20**: 148-153.

7.) Drummer, H.E., G.H. Reubel, and M.J. Studdert (1996). Equine Gammaherpesvirus 2 (EHV2) is Latent in B Lymphocytes. *Archives of Virology* **141**: 495-504.

8.) Saiki, R.K., D.H. Gelfand, S. Stoffel, et al. (1988). Preimer-directed enzymatic amplification of DNA with a thermostable polymerase. *Science* **239**: 437-441.

9.) Pereira, L. Function of glycoprotein B homologues of the family *herpesviridae*. *Infectious Agents and Disease* **3**: 9-28.

10.) Chomczynski, Piotr and Nicoletta Sacchi (1987). Single-step Method of RNA Isolation by Acid Guanidinium Thiocyanate-Phenol-Chloroform Extraction. *Analytical Biochemistry* **162**: 156-159.

11.) Meltzer, Stephen J., Shrikant M. Mane, Patrick K. Wood, Larry Johnson, and Samuel W. Needleman (1990). An Improvement of the Single Step Method of RNA Isolation by Acid Guanidinium Thiocyanate-Phenol-Chloroform Extraction. *Biofeedback* **8**: 148-149.

Detection and Localization of Human Papillomavirus Type 16 by DNA-DNA In Situ Hybridization using Biotinylated Probes and a Catalyzed Amplification System

Richard S. Lum

Supervised by Bruce R. Smoller, MD, Departments of Dermatology and Pathology, University of Arkansas for Medical Sciences, Little Rock, Arkansas

Introduction:

The human papilloma viruses (HPV) are pandemic DNA viruses (Hood 1990). Recently, using modern molecular methods 67 types of HPV have been identified. Most HPV types cause various verrucae (warts) and are spread through casual contact; types 6, 11, 16, 18, 31, 33, and 51 cause condyloma acuminatum and cervical and vaginal atypias and are spread though sexual contact. HPV types 16, 18, 31, 33, and 51 have been associated with various forms of carcinoma cancers (Elenitsas 1990). Like other herpesviruses, papilloma virus can remain latent and can never be completely eradicated from the host.

Genomic DNA of HPV-16 and HPV-18 are found more commonly in invasive cancers than DNA of other HPV types. HPV-16 and -18 infection cause abnormalities in squamous cells and cervical neoplasms, which can lead to squamous cell carcinoma, which accounts for approximately 85% of cervical cancers (Fields 1996), investigators have identified several major cell lines which contain genomic DNA of HPV-16 and HPV-18: HeLa contains 25 copies of HPV 18, SiHa contains 1 to 2 copies of HPV-16, and CaSki contain approximately 600 copies of HPV 16 (Fields 1996).

The DNA probes used in this study were prepared from sub-genomic clones of HPV cloned into plasmid vectors. All of the probes (300-500 base pairs in length) target the E5, E6, L2 open reading frames, and the upstream regulatory regions (figure 1) of HPV types 6, 11, 16, 18, 31, 33, 35, 45, 51, and 52. The probes were obtained from DAKO Corporation biotinylated and diluted in a hybridization solution containing 50% formamide, 2X standard saline citrate buffer (SSC), and sheared salmon sperm DNA.

A number of methods have been used to detect human papilloma virus (HPV) infection. The specificity and sensitivity of visual, smear, and serological methods, as well as several DNA tests--Southern blot, dot blot, polymerase chain reaction, and solution hybridization--vary from poor to high, but the more sensitive and specific tests are coupled with difficult or long protocols (Johnson 1995). All of these methods also rely on unfixed specimens only a few hours old. DNA-DNA in situ hybridization, however, provides a highly specific and sensitive DNA test which, under optimized conditions, can detect a single genomic strand (larger than 150 base pairs in length) in a few hours and with specimens that have been formalin fixed and paraffin embedded (for up to several years.)

The DNA-DNA in situ hybridization technique described in this report allows for a highly sensitive method for detecting viral DNA in routine biopsy tissues. The catalyzed signal amplification used in this technique can detect a single copy of the target genome sequence in situ. Under optimal stringency, the high specificity of DNA-DNA in

situ hybridization can detect, localize, and type viral DNA within human tissue biopsies. This information can be a valuable tool for persons infected with oncogenic associated viruses.

Materials and Methods:

The specimens were taken from routinely processed formalin-fixed paraffin-embedded biopsy tissues and prepared in DNase-free conditions. Four mm-thick sections were cut from the tissue blocks and attached to coated slides (Fisher 12-550). The slides were baked at 55°C overnight and stored at room temperature. The specimens were deparaffinized and rehydrated through a series of xylenes, absolute ethanol, 95% ethanol, and deionized water.

The pretreatment of the specimens consisted of high temperature antigen retrieval and proteolytic digestion to reverse the effects of formalin fixation. Briefly, the slides were immersed in polypropylene Coplin jars containing citrate buffer (0.1 M citric acid and 0.1 M sodium citrate pH 6.5) and incubated at 95°C for 20 minutes in a water bath. The slides were rinsed with deionized water and incubated with Proteinase K (diluted 1:5000 in 50 mM Tris-HCl, pH 7.6) for 5 minutes at room temperature. After rinsing the slides with deionized water to stop the enzymatic digestion, endogenous peroxide activity was quenched by incubating the slides in a 1% solution of hydrogen peroxide in absolute methanol for 30 minutes. Again the slides were rinsed well with deionized water to remove the peroxide and rehydrate the tissue.

To each tissue section 15 µl of biotinylated DNA probe (1.0 µg/mL) in hybridization solution was added and covered with a glass coverslip. To denature the DNA, the slides were placed on a heating plate prewarmed to 92° C and heated for 5 minutes. After two hours of annealing in a 37° C humidity chamber, the slides were immersed in tris-buffered saline (TBST) containing 0.1% Tween 20 to loosen and remove the coverslips. With the coverslips removed, the slides were washed in 2 X SSC buffer for 20 minutes at 50° C. Following a rinse with TBST, the slides were then incubated with horse radish peroxidase-conjugated streptavidin (SA-HRP) (10 µg/mL in TBS) for 15 minutes followed by several washes with TBST. The slides were then incubated with biotinyl tyramide (7 µg/mL in TBS) for 15 minutes, followed by washes of TBST, and incubated again with SA-HRP for 15 minutes. The slides were again washed and the chromogen three, 3'-diaminobenzidine tetrahydrochloride applied for 5 minutes. Three, 3' diaminobenzidine tetrahydrochloride is oxidized by HRP to produce a highly insoluble brown colored product. The chromogen reaction was stopped by immersion in deionized water.

The slides were counterstained with Mayer's hematoxylin (bluish-purple) and dehydrated through a series of 95% and 100% ethanol and xylenes and coverslipped.

Results:

The specimens consisted of 11 cases of condyloma acuminatum, 6 cervical atypias and two controls. Hematoxylin and Eosin stained sections of the specimens examined under light microscopy revealed viral change typical of HPV. All 17 cases and two controls were hybridized with a multiple-probe cocktail containing DNA probes for

HPV 6, 11, 16, 18, 31, 33, 35, 45, 51, and 52 (figure 2). Specimens showing positivity and the positive control were then hybridized for HPV-16 (table 1).

Only one of the 8 cases of condyloma acuminatum testing positive for HPV DNA were genotyped with HPV-16; 3 of the 6 cervical atypias containing HPV DNA, however, were genotyped with HPV-16.

The positive control consisted of formalin-fixed cells of the SiHa cervical carcinoma cell line, containing 1 to 2 chromosomally-integrated partial copies of the HPV-16 genome (Fields 1996, Yee 1985). The negative control consisted of sections from a normal cervical biopsy. Both were hybridized to HPV (wide spectrum and type 16) DNA and a plasmid probe from *E. coli* biotinylated and diluted in the same manner as previously described for the HPV probes. The SiHa positive controls show 1 to 2 localized areas of positivity within the nucleus, shown by the brown chromogen in figure 3. The negative controls showed no positivity.

Figures and Table:

Figure 1. Genome map of HPV-16. The genes are labeled E1 through E7 (early region genes) and L1 and L2 (late region genes) the LCR (long control region) contains replication and transcriptional control elements, and the promoter P97. (Adapted from Fields Virology.)

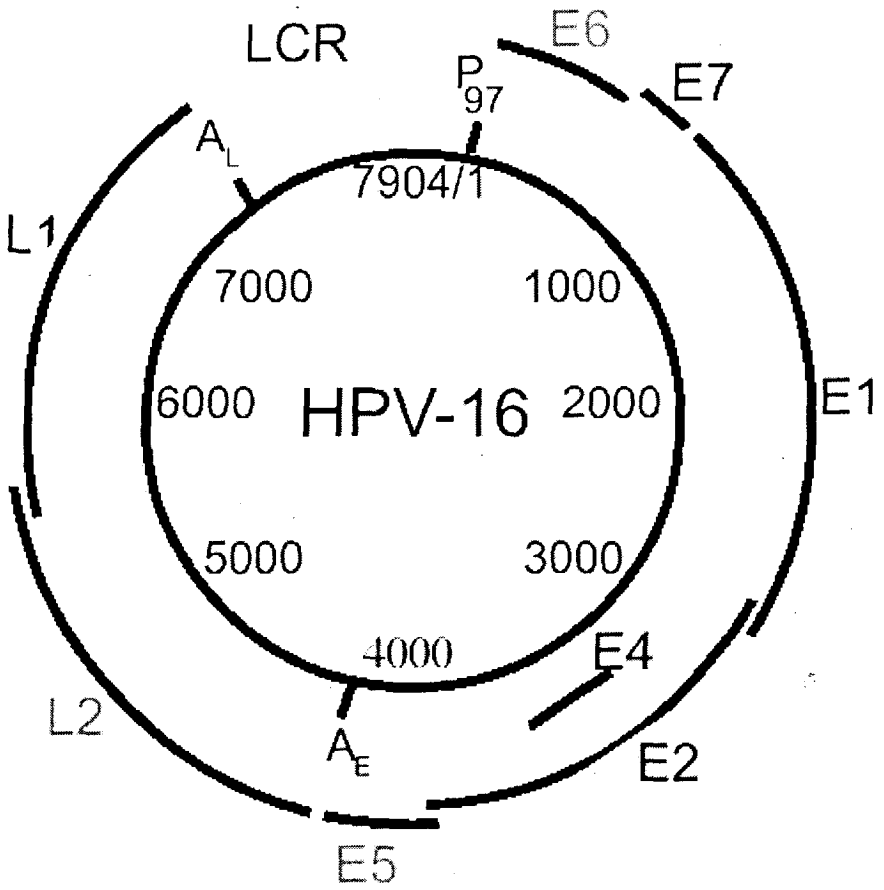

Figure 2. Condyloma Acuminatum. Koilocytes (enlarged keratinoytes) contain viral DNA fully incorporated into the host genome. Enlarged 100 x.

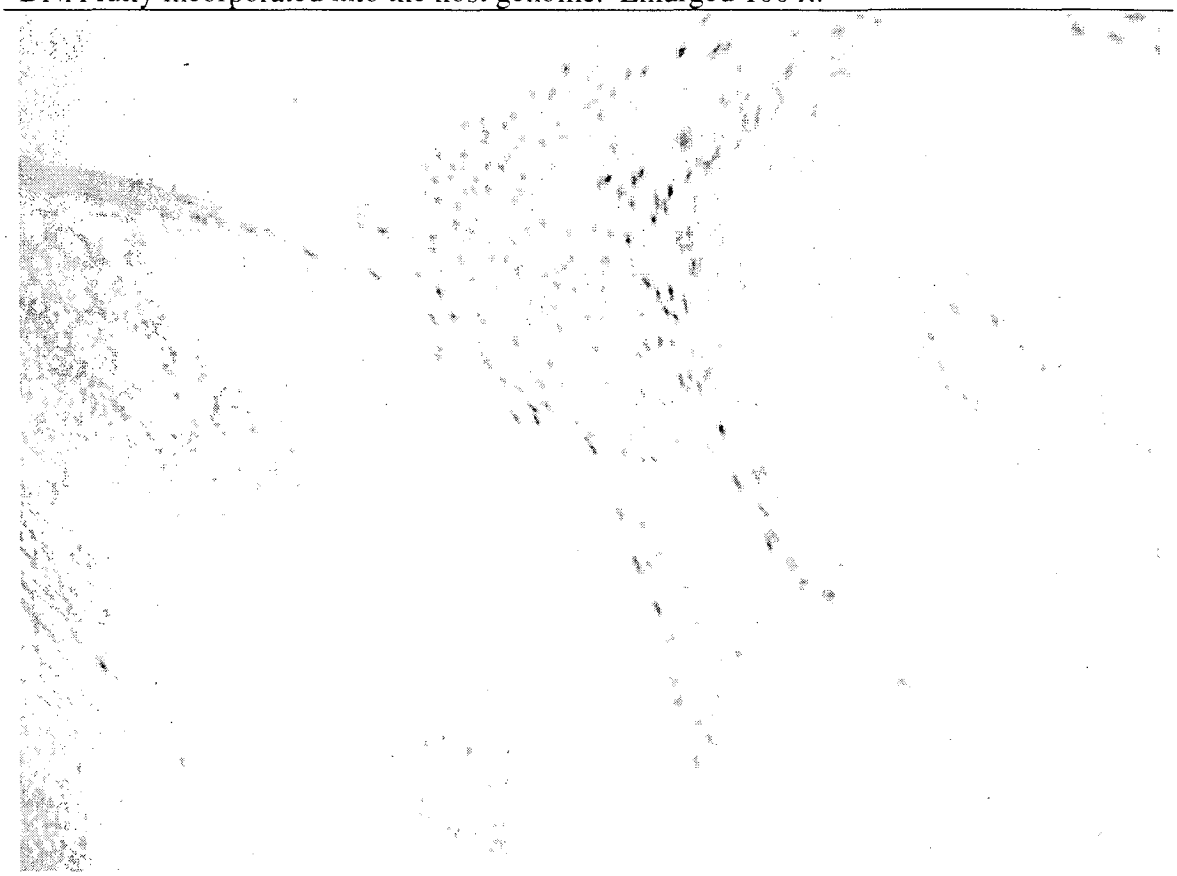

Figure 3. SiHa cervical carcinoma cells hybridized with HPV-16 DNA. SiHa cells contain 1-2 copies of chromosomally-integrated partial copies of the HPV-16 genome (Yee 1985). Enlarged 400 x.

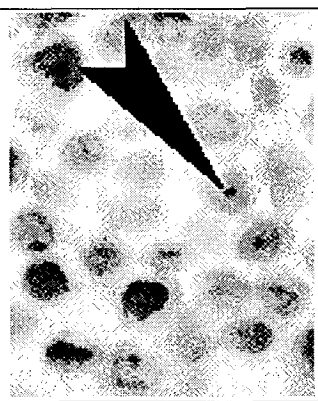

Figure 4. Malignant transformation of cells by HPV-16 and HPV-18. In a benign infection (wart), the replication of the plasmids is regulated at the same rate as the host chromosomes. If the integration of the plasmid occurs, the control of viral DNA replication is disrupted, resulting in the "unregulated production of viral replication proteins" such as the gene products of E6 and E7 which lead to higher levels of unbound p53 and Rb, which can drive the host cells into S phase, ultimately resulting in uncontrolled growth (adapted from *Molecular Biology of the Cell* (Alberts 1994).)

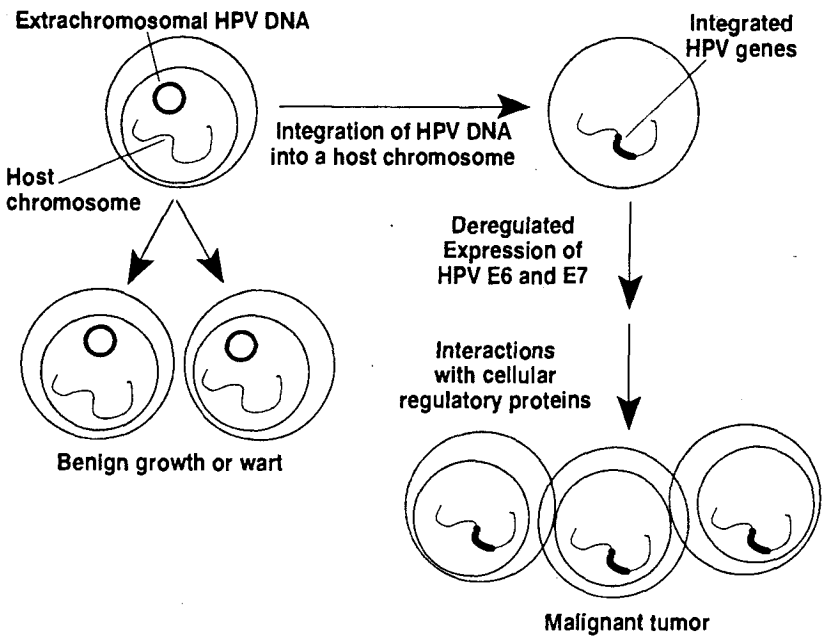

Table 1. Results of DNA-DNA in situ hybridization.

Specimen	HPV	HPV-16	Specimen	HPV	HPV-16	Plasmid
3474	+	-	5877	+	+	
4043	+	+	5879	+	-	
4741	+	-	5880	+	-	
5821	+	-	5898	+	-	
5964	-	-	5990 A1	+	+	
6124	+	-	5990 A2	+	+	
6135	-	-				
6525	+	-	Negative control	-	-	-
6528	+	-	Positive control	+	+	-
6574	+	-				

Discussion:

Genetic research has indicated that E6 and E7 gene products can jointly transform normal human cells (Münger 1989) (figure 4). Integration of the viral DNA into the host genome requires breaks--most of which occur in the E1/E2 region of the genome, resulting in a disruption and loss of function of the E1 and E2 genes and deregulation of the E6 and E7 genes, ultimately resulting in cellular transformation (Baker 1987) (figure 1).

It has been suggested that the E6 protein, which binds to the cellular p53 protein (Scheffner 1990) and the E7 protein, which binds to the retinoblastoma gene product (Rb) (Dyson 1989), exert "anti-oncogenic" influence on the genes (El-Deiry 1993, Perry 1993) by suppressing cellular division and proliferation. Loss, therefore of these E6 and E7 gene products, as the result of incorporation of viral DNA into host chromosomes and the subsequent deregulation of the E6 and E7 genes, can lead the host cells into S phase, which makes them susceptible to uncontrolled growth--cancer.

Although the exact pathway leading from infection to malignancy is not known, the ability to genotype HPV infections continues to be a good tool for the physician and patient alike to provide the best care possible. The catalyzed amplification detection system outlined in this technique provides a rapid sensitive test for the detection, typing, and localization of human papilloma virus DNA. Since the development of this technique, in situ hybridization methods have advanced from detecting many copies of HPV genomic DNA over a period of a few days (Nuovo 1990, Brigati, 1983) to this technique (which can be completed in a few hours). The specificity and sensitivity of this in situ hybridization technique, as well as it's brevity and highly reproducible results, provide a reliable test for the genotyping of HPV in cervical displasias. Perhaps further research will provide an optimized technique for DNA-DNA in situ hybridization to HPV 18, and other oncogenic associated viruses, with equally applicable results.

Literature Cited:

Alberts, B., et al. 1994. Cancer. In, Molecular Biology of the cell. 3rd Ed. Edited by B. Alberts, et al. Garland Publishing, Inc. New York. pp. 1255-1294.

Baker, C.C. et al. 1987. Structural and transcriptional analysis of human papillomavirus type 16 sequences in cervical carcinoma cell lines. Journal of Virology, 61:962-971.

Brigati, D.J., et al. 1983. Detection of viral gnomes in cultured cells and paraffin -embedded tissue section using biotin-labeled hybridization probes. Virology, 126:32-50.

Dyson, N. et al. 1989. The human papillomavirus-16 E7 oncoprotein is able to bind to the retinoblastoma gene product. Science, 243:934-937.

El-Deiry, W.S., et al. 1993. WAF1, a potential mediator of p53 tumor suppression. Cell, 75:817-825.

Elenitsas, R., et al. Diseases caused by viruses. In, Lever's Histopathology of the Skin. Edited by R. Elenitsas, et al. Lippincott-Raven Publishers. New York. pp. 578-584.

Hood, A.F. 1990. Viral Infections. In, Pathology of the Skin. Edited by E. R. Farmer

and A. F. Hood. Appleton and Lange. Norwalk, Connecticut. pp.309-317.

Johnson, K. 1995. Periodic health examination, 1995 update: Screening for human papillomavirus infection in asymptomatic women. Journal of the Canadian Medical Association, 152:483-493.

Münger, K., et al. 1989. The E6 and E7 genes of the human papillomavirus type 16 together are necessary and sufficient for the transformation of primary human keratinocytes. Journal of Virology, 63:4417-4421.

Nuovo, G.J. and Richart, R.M. Human papillomavirus DNA in situ hybridization may be used for the quality control of genital tract biopsies.

Perry, M.E., Levine, A.J. 1993. Tumor suppressor p53 and the cell cycle. Current opinions on genetic development, 3:50-54.

Scheffner, M., et al. 1990. The E6 oncoprotein encoded by human papillomavirus types 16 and 18 promotes the degradation of p53. Cell, 63:1129-1136.

Yee, C.L., et al. 1985. Presence and expression of human papillomavirus sequences in human cervical carcinoma cell lines. American Journal of Pathology, 119:3261-3266.

Cross-Sectional Geometry of the Rat Femur

Kate M.. O'Leary, under guidance of Dr. Carolyn R. Jaslow

Abstract:

The physical dimensions of a skeleton are designed to respond to many forces, including forces that occur during locomotion. The second moment of area (*I*) of limb bones is critical for resisting bending forces during locomotion. Our goal was to test the hypothesis that *I* would be greatest at the midshaft of a limb bone, where maximal bending forces are expected to occur. Femurs of nine rats were sectioned at five locations from proximal to distal. At each location a slide was made of the bone cross-section. Images of the sections were scanned into a computer, and *I* was determined. Second moment of area was significantly different among the bone locations, however, it was significantly lower at the midshaft than at the proximal end of the bone. These results suggest that *I* is not necessarily greatest at the region of maximal bending force during locomotion, reflecting other functional demands on the bone.

Introduction:

Skeletons of vertebrates are dynamic structures which must act to support gravitational loads and to withstand the forces exerted on them. Skeleton mechanical structure is crucial for withstanding forces of locomotion, forces due to rapid acceleration and deceleration, that expose the skeleton to the stresses of bending in the basic structure and torsion that may cause failure in buckling (Schmidt-Nielsen, 1984). Because an animal's skeleton must regularly resist various forces imposed upon it, it seems likely that skeletal design will reflect the need to support these forces effectively.

Studies have shown that the limb bones of various animals are most often subjected to bending forces due to movement and locomotion, because it concentrates force at the external surface of bone structure; compressive and torsional loads are usually much less (Biewener, 1982). Because of these different kinds of stresses that bones may experience, other studies have attempted to correlate structural features of bones with the kinds of forces that they experience. For example, if a bone experiences a force that is purely compressive, its shape does not matter. The most important aspect of the bone is its cross-sectional area. By contrast, if the bone is subjected to forces which cause bending in the basic structure, the shape of the bone does matter, and the value of second moment of area becomes very important. Second moment of area (I), a function of how far the material of cortical bone is distributed from the middle or neutral axis of the bone, is important for bone strength and resisting deformation. This explains the significance of second moment of area as a factor for resisting the forces of bending, rather than purely compressive forces.

According to Bertram and Biewener (1988), there is a possibility that the curvature inherent in most bone structure with some degree of bending is a "mechanically desirable loading configuration" for withstanding the forces of locomotion. If bending optimizes bone form to meet the demands for bone strength and if bones are modeled so as to promote bending in the direction of the bone which provides enough strength to

prevent buckling, it would seem logical that bones are designed to somehow resist an applied force where the most bending would occur, at the midpoint (Bertram and Biewener, 1988). So, a bone structure that is not of a radially symmetric cross-sectional shape would present a mechanism by which the bending direction of a bone may be controlled (Bertram and Biewener, 1988). Since a bone with a non-circular cross-section would most likely have bending occurring in the direction in which the bone's cross-section has the smallest second moment of area, we see that the value of the second moment of area becomes very important in determining the strength of individual bones (Bertram and Biewener, 1988).

The formulae important for understanding the relationship between the second moment of area and bending forces are **My/I=bending stress** and **I=pir^4** where *M* is the bending moment (which is a measure of force times distance), *y* is the distance from the neutral axis to the bone section edge, *I* is the second moment of area, and *r* is the radius of a nearly circular bone. According to Wainwright et al. (1982), the first formula shows that the only way to minimize the stress-induced bending of a material is by increasing the value of *I*, the second moment of area, or by decreasing the value of *y*. The second formula shows how *I* relates to the actual measurement of the bone section. It is important to note that this formula is only an example of a formula for circular structure; there are other formulae for different-shaped structures. Secondly, it is important to realize that this formula shows that *I* is proportional to length raised to the fourth power (here the radius raised to the fourth). Therefore, if the radius of a bone is only slightly increased, the bone's ability to withstand bending stress is greatly enhanced.

The purpose of this study was to test the hypothesis that second moment of area will be greatest around the midshaft of the bones, where maximal bending force is likely to occur.

Methods:

For this study, the left femur was removed from each of nine rat skeletons, and a line was drawn on each bone along its anterior edge. Each femur was embedded in a resin block, and 1-2 millimeter thick cross-sections were removed for five locations along the diaphysis of the bone, as shown in Figure 1. Each cross-section was glued to a slide. An Olympus dissecting scope equipped with a drawing tube was then used to obtain enlarged drawn images of each bone cross-section. It is important to note here that at the proximal parts of the bones, much spongy bone was visible; since spongy bone with its fibers and trabeculae is different from the dense and compact cortical bone, it could not be assumed that these materials would act in the same way when resisting bending. In the drawings, the spongy bone was included only as part of the lumen to ensure use of only areas of comparable material (the cortical bone) for determining the *I* values. When magnified drawings were completed, they were scanned so that they could be opened in the MacMoment computer program and *I* and cross-sectional area values determined. Because it was uncertain about the accuracy of the anterior edge drawn on each bone, the bone images were rotated left or right about the original a-p axis for a distance equal to 10% of the medio-lateral bone width. Each of these rotated images, in turn, were also entered into the MacMoment program and appropriate measurements determined and recorded. For all original and rotated images, statistical data were computed.

Figures and Tables:

Fig. 1: Diagram of a Rat Femur in Lateral View, showing the Locations of the Cross-Sectional Cuts

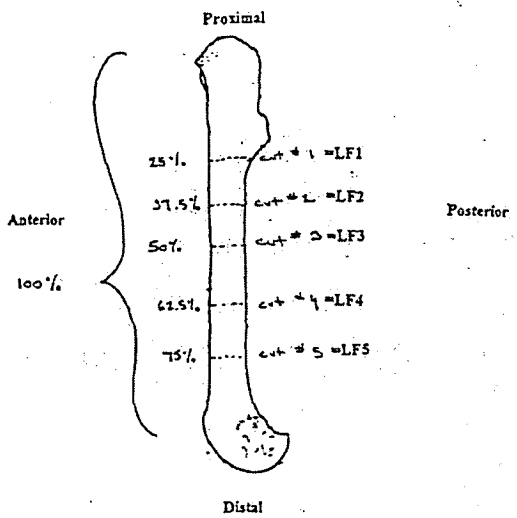

Fig. 1: Percentages listed are based on length of the entire bone, including the epiphyses.

Figure 2: I at Different Bone Sites

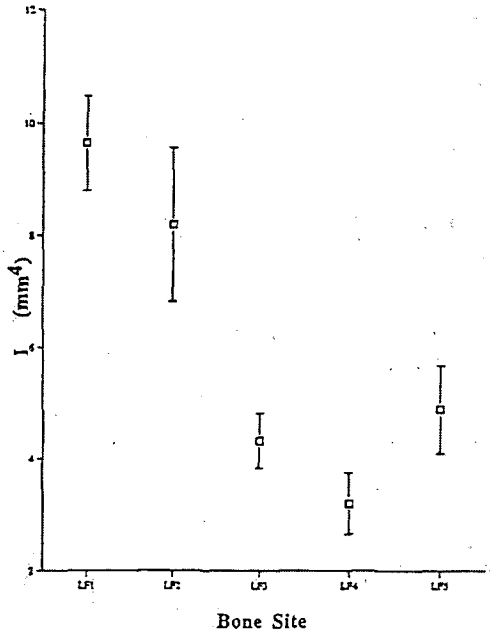

Fig.2: I at different sites along the diaphysis of the rat femur. Boxes are means for nine rats, and bars equal ±1 standard error. Abbreviations for bone sites are from Fig. 1, which shows their locations from the most proximal (LF1) to most distal (LF5).

Figure 3: I at Different Bone Sites for Left Rotation

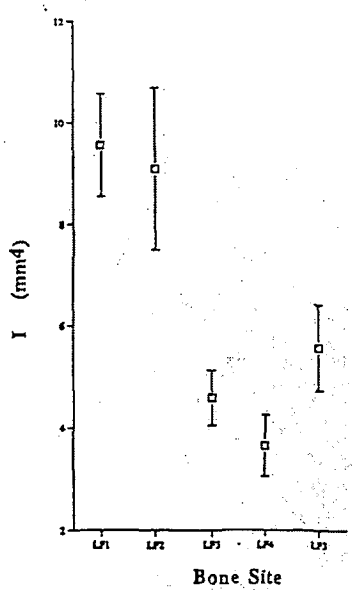

Fig.3: I at different sites along the diaphysis of the rat femur after 10% rotation to the left. Boxes are means for nine rats, and bars equal ± 1 standard error. Abbreviations for bone sites are from Fig. 1, which shows their locations from most proximal (LF1) to most distal (LF5).

Figure 4: I at Different Bone Sites for Right Rotation

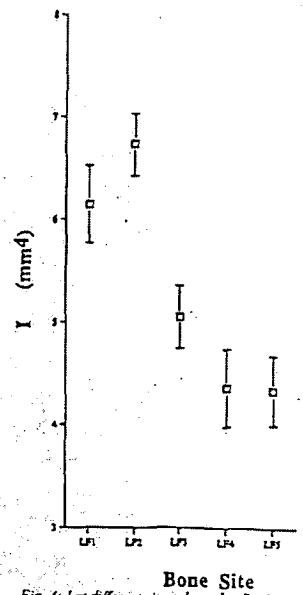

Fig. 4: I at different sites along the diaphysis of the rat femur after 10% rotation to the right. Boxes are means for nine rats, and bars equal ± 1 standard error. Abbreviations for bone sites are from Fig. 1, which shows their locations from most proximal (LF1) to most distal (LF5).

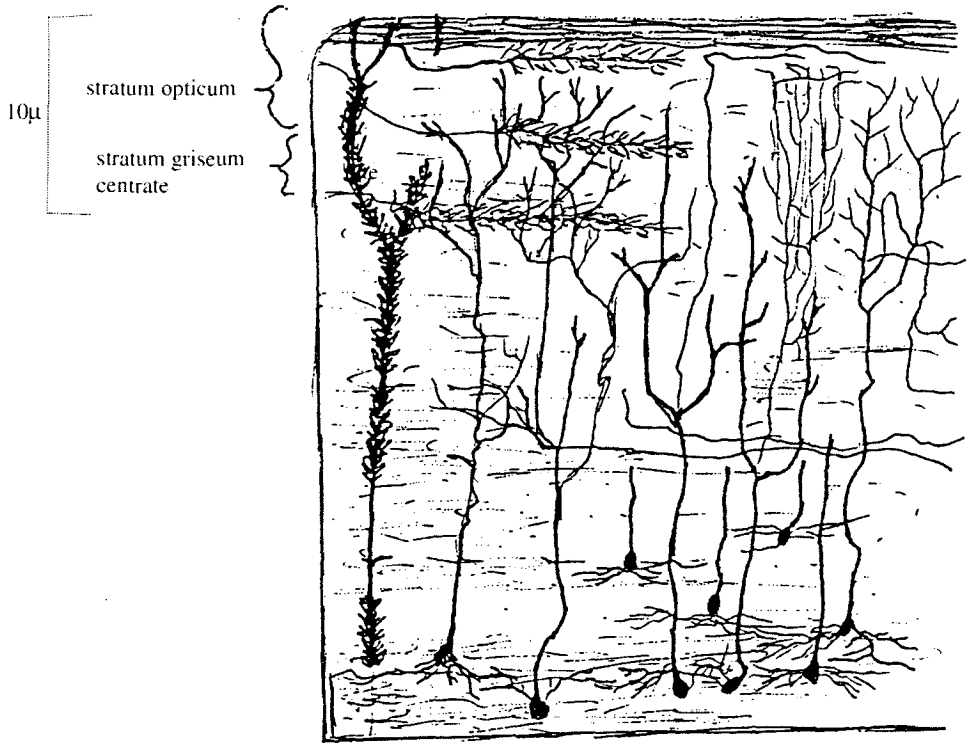

Text Figure 1

Methods:

The general protocol of this experiment is based on an experiment entitled, *Frog Optic Tectum Retinal Processing of Visual Form* by Oakley and Schafer, (1978).

The frogs are anesthesited during surgery using MS-222 (tricaine), and paralyzed to prevent muscle contractions with tubocuraarine chloride. To expose the optic tectum, the frog is placed on a board with the front jaw immobilized with an alligator clip. A cotton ball is inserted into the mouth to make the eyes bulge and the tectum rise. A square patch of skin is removed between the two tympanic membranes (fig. 7.6-3). In order to get access to the tectum the skull must be removed. This is done with the use of a dremmel tool. Once the skull is removed and the optic lobes visible, two layers of meninges must be removed. This is the most difficult part of surgery and great care is taken to prevent damaging the tectum. The remaining membranes on the optic lobe need to be parted with the use of #5 forceps to allow for the microelectrode to be admitted into the optic tectum. Great care is also taken while performing this part of the surgery and therefore is conducted with the use of a dissecting microscope. A tungsten microelectrode

is used to detect the neural responses of the frog optic tectum. The microelectrode is attached to a preamplifier. Measurements of the frequency of action potentials are recorded by the Mac lab oscilloscope and the audio amplifier that are connected to the out-put of the preamplifier. The body of the frog will be kept moist with a damp towel of MS 222, taking care not to wet the optic tectum. Frog saline is used to prevent the tectum from drying out. A reference electrode is inserted into nearby tissue and a ground electrode is attached to a front limb. Using a micromanipulator, the microelectrode is then inserted into an optic lobe. Most optic nerve fibers cross over completely. When recording information from the left eye the microelectrode should be inserted into the right optic lobe, and visa versa. Recording of optic activity will be made from several depths within the optic tectum.

In this experiment the testing of action potentials is restricted to the stimulus of an index card with a black circle of 1 inch in diameter. The index card is passed in front of the frog in a circular motion at a constant speed so that the motion stays consistent throughout the entire experiment.

Results:

Throughout the duration of the experiment only the left optic tectum was used. All frogs in which stimulus evoked Action Potentials in the optic tectum had a visual field of about 120° with vision extending to almost 90° above them. This was determined by means of an index card (stimulus) completing a half circle of motion with an original radius of larger than 120°. None of the subjects showed any response to nonvisual stimulus. Depending on the location of the electrode, action potentials peaked at various locations of the index card. It also important to note that the experiment took place in a dimly lit setting to decrease the amount of electrical interference. This could affect the excitability of some ganglion cells when stimulus is given and therefore their corresponding parts in the optic tectum would not be excited, giving no recordings. In order to effectively map the optic tectum it was visually broken up into four quadrants (Figure 1). Systematic probing of each quadrant was then conducted, starting first with quadrant one and finishing with quadrant four. In order to measure the depth of the electrode the fine tune control on the micromanipulator was used.

Quadrants I and IV showed little activity when visual stimuli was given. Throughout these areas of the *stratum opticum* and the *stratum griseum centrale,* no appreciable spikes were recorded on the Mac Lab oscilloscope. This is very unusual since it would be expected that the axons would branch evenly throughout the tectum. There is no previous documentation to be found that agrees or disputes this result; though there are many authors that write as if there is some sort of continuity throughout the layers of the optic tectum (Maturana et al., 1960, Liege and Galand, 1971, and Lazar and

Szekely, 1969, Knudsen, 1982). Only Maturana has published work using *Rana pipien* and this could be a issue of organismal physiology. Further study will have to reveal whether quadrants I and IV do contain active neurons and axons or whether they are void of these.

Within quadrants II and III all of the action potentials were recorded. Specifically in the *stratum opticum* and the *stratum griseum centrale* is where I recorded all of my data. The spikes where exclusively triphasic. These results correspond with the results taken by Maturana et al. from the optic nerve. The depth of the results indicate that they lie within the layers which hold the five functional classes of axons coming from the ganglion cells. Knowing that the majority of the axons in the optic nerve are not efferent cells the recording are not from axons of tectal origin (Maturana et al., 1960, Lazar and Szekely, 1969). It also confirms that the axons branch in this area giving a clutter of spikes rather than one distinct spike, as would occur if a reading was taken from an axon of tectal origin.

The normal oscilloscope reading with no stimulus shows a semi constant pattern of peaks and valleys (Figure 2A & C). In the extreme upper right hand corner of quadrant III action potentials can be recorded at the depth of 45μm (Figure 2B). The stimulus needed to produce action potentials comes when the index card first enters the visual field behind the frog. The burst are first very quick then slow a bit as the stimulus crosses the field of vision. The burst then stop when the stimulus is removed. These readings correspond to other reading taken in optic tectum at the same depth. All of these recording were taken in quadrants II and III. The sample shown is of the one with the greatest frequency and clarity.

At this same location the depth of the electrode was moved down to 80μm. Similar results were taken with a few exceptions. First the frequency was not quite as great when the stimulus obtained a maximum response. The stimulus was most effective at the when moved at an angle above and in front of the frog. Once again the burst continued as the index card was moved through the visual field, but once it was removed the burst stopped.

The next location where activity was found is on the boarder of the quadrant's II and III right next to the edge of the tectum. Small burst were found at the level of 40μm but the best reading were taken at a depth of 84μm. These reading were very similar to the ones taken at the same depth in other locations. Stimulus was greatest from the frontal area and it remained as long as the stimulus did. This leads me to believe that they are recording from the same ganglion cells believed to be the convex edge detectors.

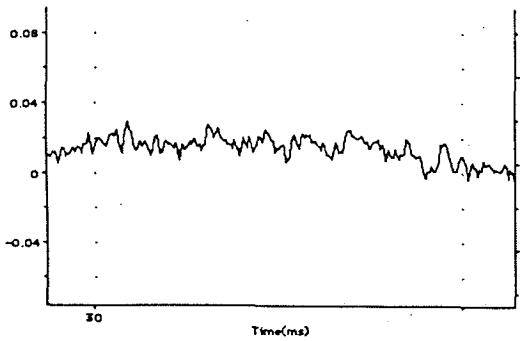

Firgure 2A: Normal Reading/No Stimuli

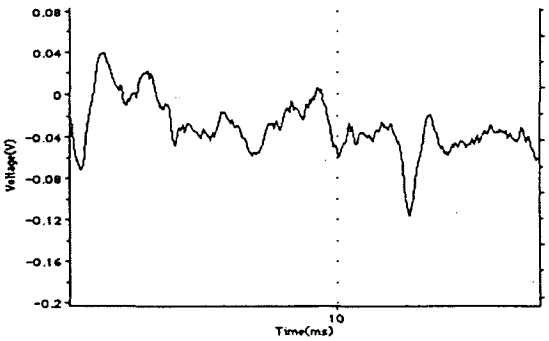

Figure 2D: Depth 80μ/Near edge of quad. II and III/Stimulus front

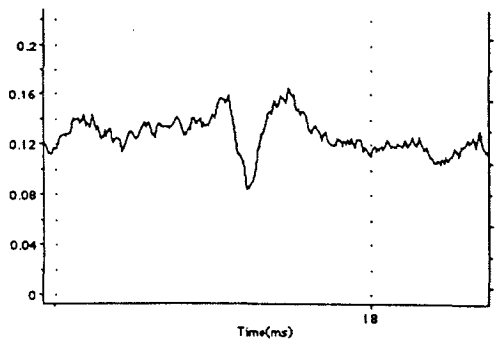

Figure 2B: Depth 45μ/Near center of optic tectum/Stimulus rear

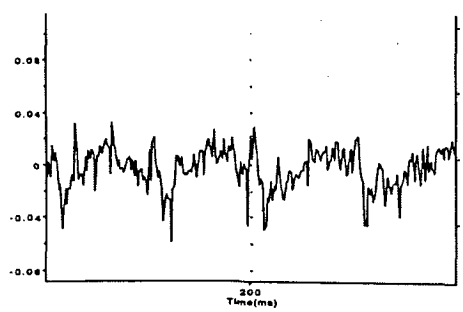

Figure 2C: Normal Reading/No Stimuli

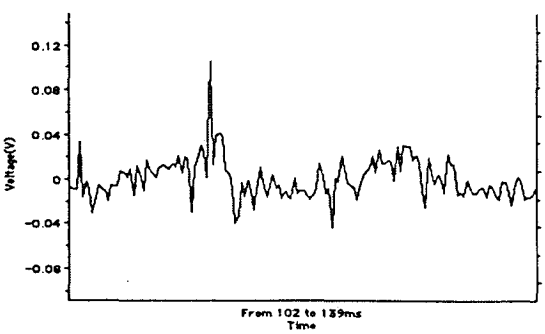

Figure 2E: Depth 84μ/Near edge of quad. II and III/Stimulus lower front

Discussion:

The ganglion cells form five distinct classes: (I) Sustained edge detectors; (II) Convex edge detectors; (III) Changing contrast detectors; (IV) Dimming detectors; (V) Dark detectors (Lettvin, et al., 1959; Maturana, et al., 1960; Lettvin, et al., 1961). It class of cells travels into a different layer of the optic tectum with the exception of III and V, which terminate on the same layer (Maturana, et al., 1960). Lazar (1969) describes the consistency of the optic tectum as layers. The first layer starts at about 30μm underneath the surface. The second layer is separated by an indistinct zone containing fewer optic terminals. The combination of two layers go down about 90μm. These two zones are rich in fine unmyelinated optic fibers. These types of fibers reflect the branching of the axons discussed early. These layers correspond to the *stratum opticum* and the *stratum griseum centrale*. The third layer contains fibers that are thicker and mostly myelinated. This layer extends down to 200μm below the surface. Underneath this layer is the fourth and final layer. This layer contains the coarsest optic fibers and the fewest (Lazar et al., 1969, Maturana et al., 1960).

The further down one goes with the electrode the less likely they are to find action potentials. This is due to the lack of branching and the coarseness of the fiber (Lazar et al., 1969). Instead of recording a general area one must have the electrode touching an axon and must properly be stimulating the subject. If an electrode passes through the first two layers it can be withdrawn back to that area and still record. This is because it is recording from many axons in the area and doesn't actually have to touch them. Within the lower levels of the tectum once the electrode has passes a point it can never get a reading from that same axon, since it had to destroy it to get a reading from it. This could be a reason for the lack of recordings coming from the deeper levels.

When recording in the first layer of the tectum we encountered the greatest amount action potentials. This was expected, but what wasn't expected is that all of the recording came from quadrants II and III. By looking at physiological reports given by Maturana et al. (1960) of *rana pipiens* it is easily seen that the axons branch throughout the entire surface of the tectum. Since the recording are thought to be taken from these branching axons it would only be logical to assume that recording could be taken from quadrants I and IV. So the easy answer that axons aren't present isn't a viable one. A more logical explanation may be from experimental technique. When removing the meninges I used a little pin with a hook on the end of it. I would hook and tear the meninges off, always starting from the point at which the left and right optic tectums meet. If the hook penetrated the meninges too far than it would puncture and tear tissue in the optic tectum. The majority of the time this did not seem to happen because no blood was present at the removal of the meninges. This is also a doubtful since the tissue underneath should have remained intact, but no recording were able to be taken from there.

With the exceptions of quadrants I and IV the recordings taken at a level of 30μm to around 50μm showed that when the stimulus entered the visual field a burst of activity with a high frequency was recorded. The frequency slowed, but did not stop, as the stimulus crossed the visual field. This is consistent with the findings given by Maturana et al. (1960). This field represents the first class of ganglion cells, sustained edge

detectors. When an object darker or lighter than the background enters the visual field the ganglion cells start firing constantly off action potentials that are being received and recorded in the tectum. These cells are not affected by the conditions of light unless it is completely dark (Maturana et al., 1960). This is important to note since this experiment was only conducted in a dimly lit area.

A similar response was recorded at the level around 50μm to 90μm. The frequency of the spikes are not as great as those recorded at shallower depths. The stimulus had the greatest affect when it crossed the center of the visual field. Once again the action potentials were sustained throughout the duration that the stimulus was in the visual field. This time the frequency of the action potentials decreased at a larger scale than before. Maturana's (1960) describes this as class II convex edge detector. Cells in that fall into class II are also not affected by the condition of light (Maturana et al., 1960).

References:

Koskelainen, A. Hemila, S. Donner, K., 1944. Spectral sensitivities of short- and long-wavelength sensitive cone mechanisms in the frog retina. *Acta Physiol Scand.* **152 (1)**:115-124.

Knudsen, 1982. Auditory and Visual Maps of Space in the Owl's Tectum. *J. Neuroscience* **2**:1177-1194

Lazar and Szekely, 1969. Distribution of Optic Terminals. Brain Res. **16**:1-14

Liege, B., Galand, G., 1971. Single-Unit Visual Responses in the Frog's Brain. *Vision Res.* **12**:609-22

Maturana, Lettevin, McCulloch, Pitts, 1960. Anatomy and Physiology of Vision in Frog. *J. Gen. Physiol.* **43**:127-170

Oakley, B. and Schafer, R., 1978. *Experimental Neurobiology: Frog optic tectum*, Oakley and Schafer (ed.), The University of Michigan Press, Michigan, pp. 239-246.

A Characterization of Laminarinases Secreted by *Achlya ambisexualis*

A. J. Robison

Abstract:

Mycelial colonies of the common water mold *Achlya ambisexualis* were grown in liquid medium and exposed to peptone, which induces hyphal branching. During the period of branching, secretion of enzymes capable of degrading the glucose polysaccharides that make up the cell walls of the fungi was monitored. Laminarin (a polysaccharide containing both b-1,3 and b-1,6 linked glucose molecules) was used as a substrate for laminarinase tests, and activity was assayed by measuring the release of reducing sugars with a neocuproine assay. The enzymes' optimum temperature, optimum pH, and substrate specificity (pure b-1,3 as opposed to pure b-1,6) were determined. Comparisons were made with laminarinases harvested from *A. ambisexualis* under other conditions, including normal growth, and osmotic stress.

Introduction:

Oomycetes are primitive eukaryotes grouped with the fungi because, like most fungi, they exist in the form of hyphae: long, finger-like cells that are capable of invading food sources to absorb nutrients from within. The growth of these organisms involves outward turgor pressure pushing against the cell wall of the hyphae. As long as the apices of the hyphae are kept slightly plastic (malleable), elongation continues and the organism grows. Branching begins laterally in the older regions of hyphae where the cell walls have reached their normal, rigid state. In order for branching to occur, the cell wall in the area of branch formation must be softened so that the internal turgor pressure of the organism can force the wall outward, and a new apical tip can form. To cause this increase in plasticity in the cell wall, the organism is thought to secrete hydrolytic enzymes which break down some of the materials that make up the wall in the areas at which growth is to occur. This process has been previously studied in one common Oomycete, *Achlya ambisexualis*, with regard to enzymes that break the b-1,4 linkages in glucan chains (6). However, the complex matrix of the fungal cell wall also contains b-1,3 and b-1,6 linked glucans (9), and the breaking of these linkages has not been previously studied with regard to its correlation to branching in *Achlya*. The effect of b-1,3 glucanases on the morphogenesis of some fungal cells (3,4,5,8), on the walls of young cereal plants (7) and their use as a plant defense mechanism against fungal parasites (1) have been noted in the past, but their role in the morphogenesis of *Achlya ambisexualis* has not previously been studied, and no attempt to characterize or isolate these b-1,3 glucanases from the organism during branching has previously been made. The purpose of this study is to determine whether enzymes that are capable of hydrolyzing these differently linked glucans are secreted by *Achlya* during branching.

Materials and Methods:

A culture of *Achlya ambisexualis*, strain E 87 male, was grown on PYG agar at room temperature. Twenty-four plugs of agar, approximately 0.5 cm2, were removed aseptically from the periphery of the colonies after approximately four days of growth. They were placed in 10 mm Petri plates filled with approximately 25ml defined liquid growth medium (6), four to a plate, and allowed to grow for four days at room temperature. To induce branching, the exhausted medium was replaced with salt medium containing all of the inorganics in the defined medium as well as 0.2% peptone. Control cultures were given 25 ml fresh growth medium instead of the peptone solution. All cultures were incubated at room temperature up to five hours, and branch induction was observed in experimental peptone treated cultures beginning at two hours and increasing for the duration of the five hour period. Control cultures did not exhibit a comparable level of branching.

Each hour, 1 ml samples of the media were taken from both the control and experimental cultures and frozen pending enzyme assay. Endo 1-4 b glucanase (cellulase) activity was assayed, according to the method of Hill (6), in order to verify that already studied wall-softening enzymes were being secreted. Laminarinase activity was assayed using laminarin (a b-1,3 and b-1,6 linked glucan) as a substrate. For a basic enzyme assay, samples of medium were incubated with the substrate for three hours, using a 0.05 M sodium acetate buffer of pH 5.0. Release of reducing equivalents (expressed in terms of mg glucose) from the substrate was assayed using a neocuproine assay (2).

The optimal temperature for laminarinase activity was determined by incubating the already described reaction mixtures at the following temperatures: 15°C, 25°, 30°, 35°, 40°, 45°, 50°, and 60°C. The optimal pH for laminarinase activity was determined by incubating, at 40°C, reaction mixtures whose pH values were altered with the following buffers at: glutamic acid (pH 4.0, 4.5, 5.0), histidine (pH 5.0, 5.5, 6.0), PIPES (pH 6.0, 6.5, 7.0, 7.5), Tris base (pH 7.5, 8.0, 8.5, 9.0), and glycine (pH 9.0, 9.5, 10.0). Pustulan (a b-1,6 glucan) and curdlan (a b-1,3 glucan) were also examined for possible use in assays, and these reaction mixtures were incubated at 40° C.

Laminarinase activity was also measured in *A. ambisexualis* cultures grown under osmotic stress. The enzymes in this medium were tested for activity against laminarin at 40°C and 5.0 pH. This was done in order to investigate the effects of osmotic stress on laminarinase secretion, since it has been observed in the past that cellulase secretion increases during osmotic stress (6).

Results:

Graphs 1 and 2 show cellulase and laminarinase activity in samples taken at various times in both branching (peptone) and non-branching (control) mycelia. It is important to note the extreme similarity of the pattern of secretion over time. Graph 3 shows the effect of temperature variation on enzyme activity. The peak temperature for activity appears to be 40° C, though some activity occurs at lower temperatures, and at slightly higher heat. Graph 4 shows the relative activity of the enzyme against three substrates, each with a different type of glucan linkage. Graph 5 shows the relationship

between pH and enzyme activity for three trials of each buffer type. There appears to be a clear peak at pH 6.0. In graph 6, which shows averages of the data in graph 5, the different buffers are shown as seperate lines that overlap at common pH levels. This overlapping method was used to insure that the changes in enzyme activity were the results of pH change, and not the effects of a seperate reaction with the buffers used. Graph 7 shows the results of four experiments comparing the laminarinase activity of cultures induced to branch with those grown under osmotic stress.

Discussion:

Laminarinase activity detected in the medium during branching correlated with an similar rise in cellulase activity. This is the first observation of such a phenomenon, and this observation expands the range of molecular sites within the cell wall upon which plasticizing enzymes may act.

Preliminary data on substrate specificity indicate stronger activity against the minority b-1,6 glucan linkages than against the more prominent b-1,3 linkages. This may indicate that laminarinase is secreted in order to break up the outer layers of the cell wall, which are thought to contain less cellulose and b-1,3 polymers, and more of the b-1,6 linked glucans (9). However, these results are not truly reliable due to the very different natures of the substrates involved. Curdlan is a powder that is insoluble in water, and pustulan, though soluble when heated, has a tendancy to precipitate unexpectedly. The effects of these physical properties on the ability of the glucanases to react with substrate molecules are unknown, and may have biased the assay results.

The results of testing for optimum temperature agree with the unpublished findings of Xin Du (pers. comm.), who has studied a similar *Achlya* enzyme which is not secreted like the enzyme in this study, but is found, instead, intracellularly. He presumes that the intracellular laminarinases are used for mobilizing internal food stores, and no effort has been made to correlate them with hyphal morphogenesis. Many of the studies of b-1,3 glucanases isolated from other organisms have found optimal temperatures quite different from the 40° C found in this study (3,4,5,8), but they vary both above and below this temperature, and seem to have a mean close to 35°.

The pH optimum of 6.0 was slightly higher than expected, and future experimentation will take this optimum into account by using appropriate buffer solutions during incubation periods. The pH optima of similarly studied glucanases have been found to range between 5.0 and 7.5, with little pattern with regard to the organisms from which they were isolated (3,4,5,8). Though they are varied, the optima average around 5.6 for non-cellulolytic glucanases (b-1,3's and b-1,6's), though those that cleave only b-1,6 linkages always have pH optima at or above 6.0.

The results of testing enzyme secretion in mycelia grown under osmotic stress were inconclusive. Under osmotic stress, growth is spherical, with equal wall extension in all directions simultaneously (isometric growth). If the theory of wall softening with glucanase enzymes is correct, then such growth may correlate with a greater level of enzyme secretion than normal growth or induced branching. In other studies, levels of cellulase secretion have been found to be vastly greater during growth under osmotic stress than under branching conditions (6). Because my work involves enzymes thought to share many functions with cellulases, a similar increase in laminarinase secretion was

expected. However, a comparison of enzyme activity in cultures treated with peptone and those treated with osmotic stress inducers were not consistant, often showing very different ratios of secretion between the two types of culture. These results are inconclusive, and bear further investigation.

My future investigations into laminarinase's role in hyphal morphogenesis will include a variety of experiments. The data on substrate specificity must be confirmed. In later stages of study, an electrophoretic activity assay for laminarinase will be developed in order to discover how many species of the enzyme are secreted by *Achlya*, and to determine the molecular weights of the enzymes for further characterization.

Graphs:

Graphs 1 &2: Cellulase and Laminarinase Secretion in Branching and Non-branching Mycelia

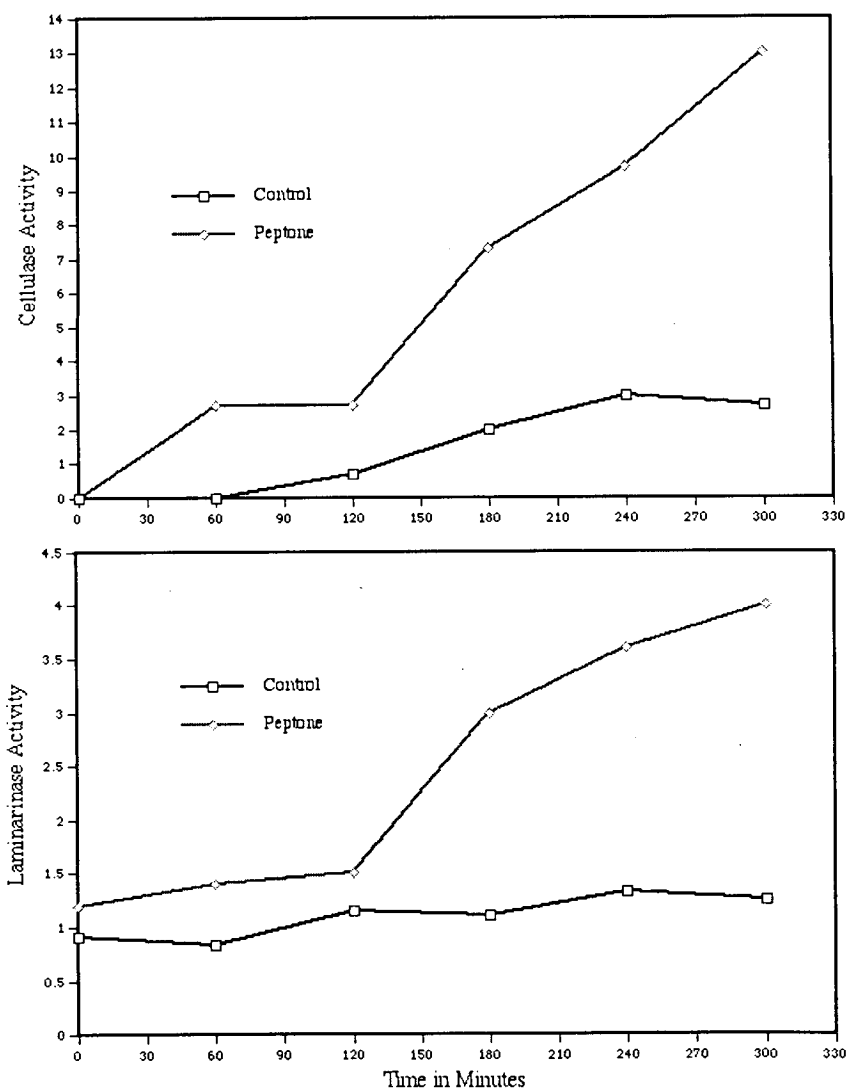

Graph 3: Effect of Temperature

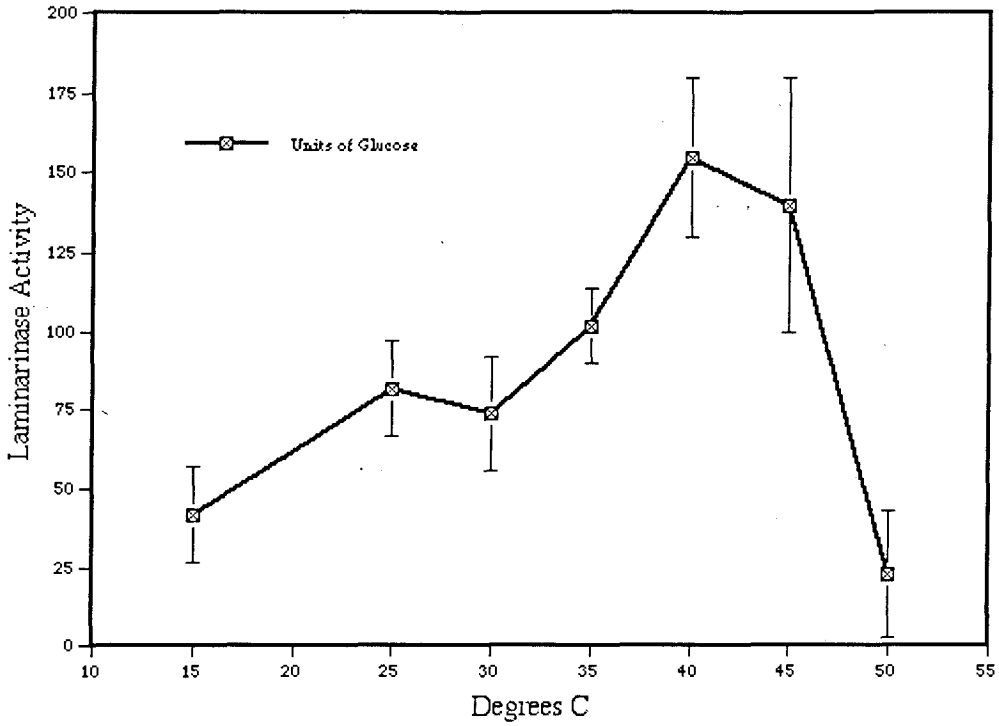

Graph 4: Comparison of Substrates

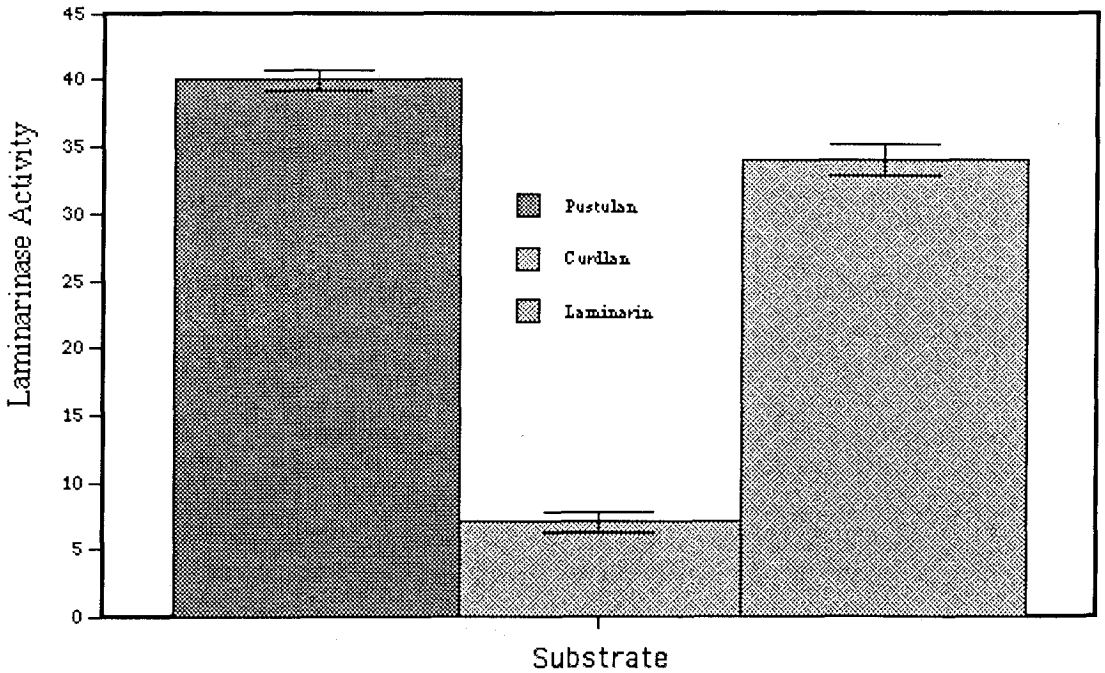

Graphs 5 & 6: pH Optimum for Laminarinase

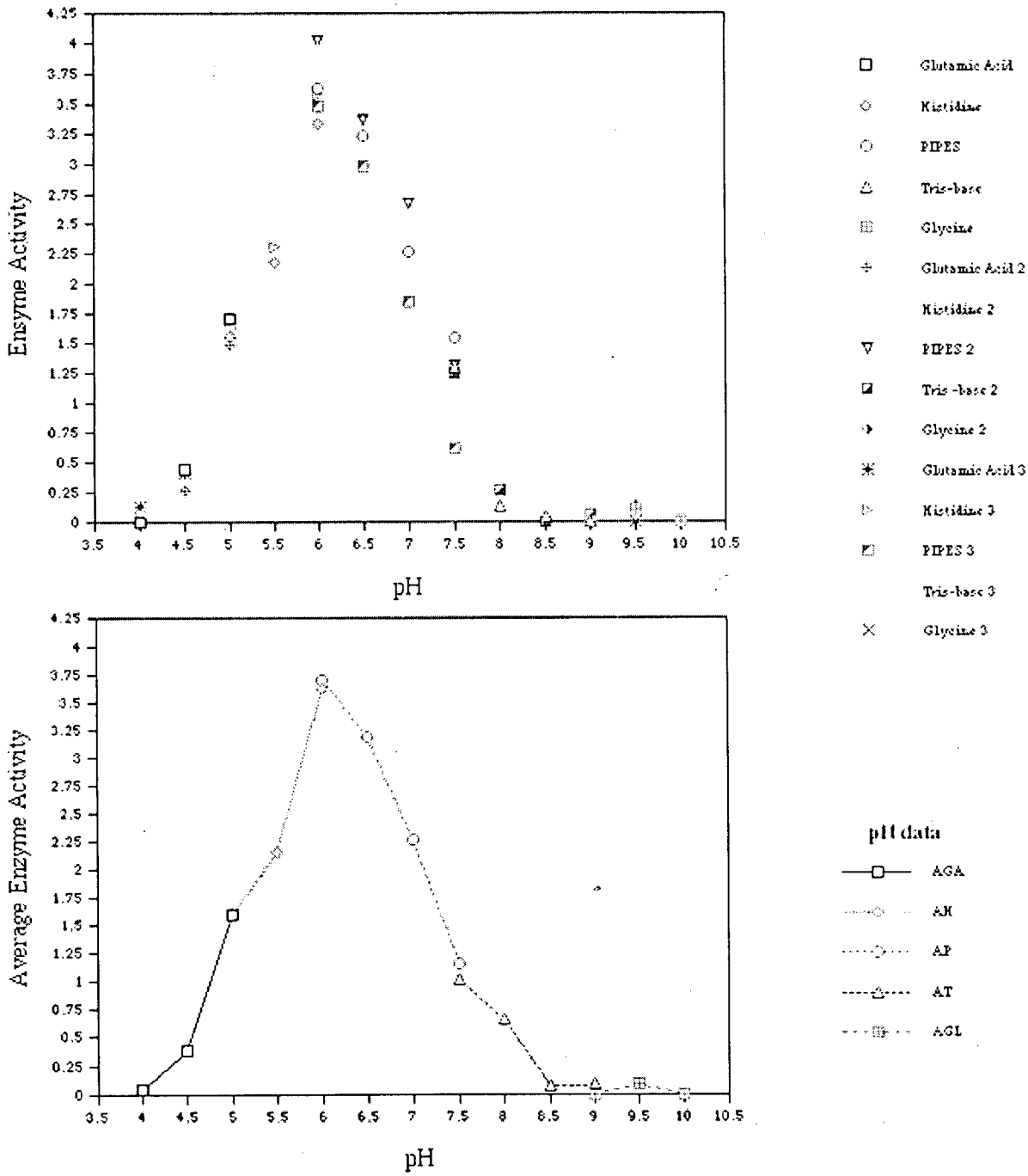

Graph 7: Comparison of Yeastoid Growth to Induced Branching

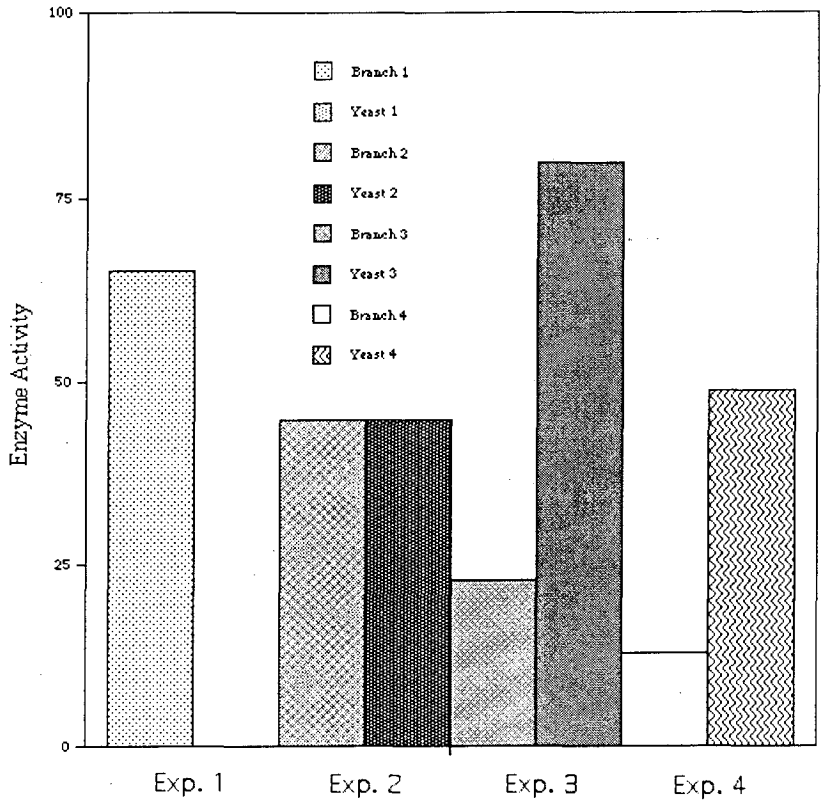

Literature Cited:

1. Daugrois, Jean Heinrich, Claude Laffite, Jean-Paul Barthe, Catherine Faucher, Andrè Touze, and Marie-Thèrèse Esquerre-Tugaye, 1992. Purification and Characterization of Two Basic b-1,3 Glucanases Induced in *Colletotrichum lindemuthianum*-Infected Bean Seedlings. Archives of Biochemistry and Biophysics, **292**: 468-474.

2. Dygert, Stephen, L. H. Li, Don Florida, and John A. Thoma, 1965. Determination of Reducing Sugar with Improved Precision. Analytical Biochemistry, **13**: 367-374.

3. Gooday, Graham W. and Neil A. R. Gow, 1990. Enzymology of Tip Growth in Fungi. Tip growth in PLant and Fungal Cells. ed. I. B. Heath. Academic Press, Inc.: Toronto, Canada.

4. Gow, Neil A. R., 1989. Control of Extension of the Hyphal Apex. Current Topics in Medical Mycology, **3**:109-152.

5. Harold, F. M., 1997. How Hyphae Grow: Morphogenesis Explained? Protoplasma **197**: 137-147.

6. Hill, T. W., 1996. Electrophoretic characterization of endo-(1,4)-b-glucanases secreted during assimilative growth and antheridiol-induced branching in *Achlya ambisexualis*. Canadian Journal of Microbiology, **42**: 557-561.

7. Kotake, Toshihisa, Naoki Nakagawa, Kazuyoshi Takeda, and Naoki Sakurai, 1997. Purification and Characterization of Wall-bound Exo-1,3-b-D-Glucanase from Barley (*Hordeum vulgare* L.) Seedlings. Plant Cell Physiol., **38(2)**: 194-200.

8. Pitson, S. M., R. J. Seviour, and B. M. McDougall, 1993. Noncellulolytic fungal b-glucanases: Their Physiology and Regulation. Enzyme Microb. Technol., **15**: 178-192.

9. Reiskind, Julia B. and J. T. Mullins, 1981. Molecular architecture of the hyphal wall of *Achlya ambisexualis* Raper. II. Ultrastructural analyses and a proposed model. Canadian Journal of Microbiology, **27**: 1100-1105.

Embryonic Leaf Number in Maize Differing in Juvenile Leaf Number

Alex Wooley, under guidance of Dr. Bruce Abedon

Abstract:

The transition between juvenile and adult vegetative phase in maize occurs between leaves five and seven. The number of juvenile leaves is comparable to embryonic leaf number which is between five and six. This has led to speculation that juvenile leaf number is directly determined by embryonic leaf number and genes active in a developing embryo. Two distinct populations derived from Minn11 (Minn11 C3 JWE and Minn11 C3 JWL) that had been divergently selected for the number of juvenile leaves were hand dissected. No difference in embryonic leaf number (5.02 and 5.01, respectively) was found although juvenile leaf number has been reported to be significantly different. Embryonic leaf number in S5 families derived from Minn11 as well as several inbreds and hybrids was also examined. No significant difference was found, with all genotypes having about five embryonic leaves. Data from the Minn11-derived populations, inbreds, and hybrids suggests that there is no correlation between juvenile and embryonic leaf number. Juvenile leaf number is not controlled by genes in a maturing embryo.

Introduction:

Maize plants have both a juvenile and adult vegetative phase. These phases can be easily identified based on leaf anatomy. Juvenile leaves produce visible epicuticular wax and have an absence of epidermal hair, while adult leaves are pubescent and lack visible epicuticular wax (Poethig, 1990). Most maize genotypes have between five and seven juvenile leaves (Poethig, 1990). This is similar to the number of leaves in a mature embryo, which has been found to be between five and six (Abbe and Stein, 1954; Hubbard, 1951). This has led to the hypothesis that the number of juvenile leaves is controlled by genes that act during seed maturation and is directly related to the number of embryonic leaves. However, *glossy15* (*gl15*), a mutation that reduces the number of juvenile leaves relative to wild-type, does not affect the number of embryonic leaves (Evans et al., 1994).

Minn11, a *sugary* corn made of 50% field corn and 50% sweet corn inbreds, has been divergently selected for the timing of the juvenile to adult vegetative transition for three generations. Minn11 displays juvenile traits (last leaf with juvenile wax) up to leaf ten, while Minn11 C3 JWE (third cycle in the early transitional direction) and Minn11 C3 JWL (third cycle in the late transitional direction) show these same juvenile traits up to leaf 7.2 and 13.2, respectively (Abedon et al., 1998). If the number of juvenile and embryonic leaves are directly related, Minn11 C3 JWE and Minn11 C3 JWL should show different numbers of embryonic leaves that are correlated with juvenile leaf number.

The purpose of this project is to (1) determine if juvenile leaf number is directly related to embryonic leaf number and, therefore, controlled by genes in the developing

embryo, in Minn11 C3 JWE and Minn11 C3 JWL, and (2) determine embryonic leaf number in nine S5 families derived from Minn11 and various hybrids and inbreds.

Materials and Methods:

For the Minn11 C3 JWE and Minn11 C3 JWL populations, 50 kernels each were evaluated for embryonic leaf number after using a balanced bulk sampling method. For the nine S5 families derived from Minn11, 10 kernels were examined per family. Five seeds each were evaluated for several inbreds (A188, A632, B37, B73, DE811, MO17, OH43, W23, W64a) and hybrids (A632 X all inbreds, W23 X all inbreds).

The number of embryonic leaves was found by hand dissection. Seeds were soaked in H_2O at 4^0C for twelve hours. Subsequently, the pericarp was removed and the kernel was cut down the middle parallel to the embryo axis. Using a dissecting microscope (30X magnification) the embryo was removed and cut in half along the embryo axis. If the cut was slightly off-center, only the side containing the apical meristem was examined. By peeling the leaves back sequentially, the total number of visible leaves was scored. There may have been one to several leaf primordia adjacent to the apical meristem that were not counted because they could not be seen at the magnification level used. The coleoptile was not scored as an embryonic leaf.

Results and Discussion:

Table 1: Mean number of embryonic leaves in Minn11

Population	Mean Number of Embryonic Leaves
Minn11 C3 JWE	5.02
Minn11 C3 JWL	5.01

For both Minn11 C3 JWE and Minn11 C3 JWL, embryos were found that contained either four, five, or six leaves. Each population had an average of five embryonic leaves (Table 1). Embryos showing only four leaves may have been miscounted because previous studies have shown that maize embryos contain either five or six embryonic leaves (Abbe and Stein, 1954; Hubbard, 1951). Alternately, sweet corn may be different than field corn in that four leaves are possible in the sweet corn embryo. By far, the majority of kernels in both populations had five leaves. Even though these populations varied greatly in juvenile leaf development (Abedon et al., 1998), there was no difference in embryonic leaf number, a result consistent with Evans et al. (1994). Consequently, the number of juvenile leaves probably is not controlled by genes during seed development and is not directly related to the number of embryonic leaves. This means that juvenile leaf number is determined post-embryonically, either by genetic or environmental stimulus, or a combination of both. Further research is needed to determine what affects juvenile leaf number.

Table 2: Mean number of embryonic leaves in S5 families derived from Minn11

Family	Mean Number of Embryonic Leaves
8813-1	5.14
8815-4	5.14
8817	5
8819-2	5
8821-1	5
8823-3	5
8825-1	4.86
8827-1	5
8831-2	5
8833-1	4.83
8835-1	5.5
8837	5
8839	6
8840	5.1
884-1	4.86
883-1	5
845-1	5.13
847-1	5

All S5 families had about five embryonic leaves per kernel, on average, except 8839 which had six (Table 2). Similar to Minn11 C3 JWE and Minn11 C3 JWL, the majority of kernels in most families had five embryonic leaves except 8839 in which the majority of kernels had six leaves.

Table 3: Mean number of embryonic leaves in various inbreds

Inbreds	Mean Number of Embryonic Leaves
A188	5.00
A632	5.00
B37	5.00
B73	5.50
DE811	5.00
MO17	5.00
OH43	5.00
W23	5.00
W64a	5.00

Table 4: Mean number of embryonic leaves in hybrids of A632 and W23

Hybrids	Mean Number of Embryonic Leaves
A632 X A188	5.00
A632 X B37	5.00
A632 X B73	5.00
A632 X DE811	5.00
A632 X MO17	5.00
A632 X OH43	5.25
A632 X W 64A	5.33
W23 X A632	5.25
W23 X A188	5.00
W23 X B37	5.25
W23 X B73	5.00
W23 X MO17	5.25
W23 X OH43	5.00
W23 X W64A	5.25

The majority of inbreds had a mean of five leaves with only one variation (B37 had a mean of 5.5). There may be several reasons for this: similar genetic constitution regarding this trait, kernels in different stages of maturation, or self pollination decreasing the chance for diversity. The latter two possibilities are unlikely. Environmental conditions can alter the degree and rate of maturation (Abbe and Stein, 1954; Sass, 1951; Stein, 1952), which may compound genetic differences. However, seed maturation differences caused by environmental variation were probably minimal in this study since all kernels were grown in the same environment and were harvested after physiological maturity.

In addition, the hybrids showed no hybrid vigor for embryonic leaf growth. Hybrids had the same number of embryonic leaves (an average of five leaves per kernel) as their parental inbred lines (Tables 3-4). The data in Table 3 provides further evidence that embryonic leaf number does not determine juvenile leaf number because several of the inbreds evaluated do not have the same number of juvenile leaves (Poethig and Passas, 1993) although they have the same number of embryonic leaves.

This research has provided further evidence that juvenile leaf number is not determined by embryonic leaf number. However, additional study involving histological examination of Minn11 C3 JWE and Minn11 C3 JWL will help to prove or disprove this hypothesis more conclusively.

Literature Cited:

Abbe, E. C., and O. L. Stein. 1954. The growth of the shoot apex in maize: embryogeny. Amer. J. Bot. 41:285-293.

Abedon, B.G., A. J. Wooley, and W. F. Tracy. 1998. Embryonic leaf number in populations differing in juvenile leaf number. p.64 In 40th Annual Maize Genetics Conference, Lake Geneva, WI (abstr.).

Evans, M. M. S., H. J. Passas, and R. S. Poethig. 1994. Heterochronic effects of *glossy15* mutations on epidermal cell identity in maize. Development 120: 1971-1981.

Hubbard, J. E. 1951. Leaf patterns i n mature embryos of inbred lines of corn. M. S. Thesis, Univ. Illinois.

Poethig, R. S. 1990. Phase change and the regulation of shoot morphogenesis in plants. *Science* 250: 923-930.

Poethig, R. S., and H.J. Passas. 1993. Phase change in inbred and exotic lines of maize. Maize Gen. Coop. News. 67:92.

Sass, J. E. 1951. Comparative leaf number in the embryos of some types of maize. Iowa State Coll. Jour. Sci. 25: 509-512.

Stein, O. L. 1952. A comparison of embryonic growth rates in two inbreds of *Zea mays* L. and their reciprocal hybrids. M. S. Thesis, Univ. Minnesota.